

A specific, glycomimetic Langerin ligand for human Langerhans cell targeting

Eike-Christian Wamhoff^{1,2}, Jessica Schulze^{1,2*}, Lydia Bellmann^{3*}, Mareike Rentzsch¹, Gunnar Bachem⁴, Felix F. Fuchsberger^{1,7}, Juliane Rademacher¹, Martin Hermann⁵, Barbara Del Frari⁶, Rob van Dalen⁷, David Hartmann¹, Nina M. van Sorge⁷ Oliver Seitz⁴, Patrizia Stoitzner³ and Christoph Rademacher^{1,2#}

*These authors contributed equally. #Corresponding author: christoph.rademacher@mpikg.mpg.de

¹Max Planck Institute of Colloids and Interfaces, Department of Biomolecular Systems, 14424 Potsdam, Germany

²Freie Universität Berlin, Department of Biology, Chemistry and Pharmacy, 14195 Berlin, Germany

³Medical University of Innsbruck, Department of Dermatology, Venereology and Allergology, 6020 Innsbruck, Austria

⁴Humboldt-Universität zu Berlin, Department of Chemistry, 12489 Berlin, Germany

⁵Medical University of Innsbruck, Department of Anesthesiology and Intensive Care Medicine, 6020 Innsbruck, Austria

⁶Medical University of Innsbruck, Department of Plastic, Reconstructive and Aesthetic Surgery, 6020 Innsbruck, Austria

⁷University Medical Center Utrecht, Utrecht University, Medical Microbiology, 3584 CX Utrecht, Netherlands

Supporting Information

Supporting Notes	S2
Supporting Figures	S3
Supporting Tables	S16
Supporting Schemes	S18
Methods	S21
Supporting References	S54

Supporting Notes

Note S1

Upon titration with both GlcNS analogs **2** and **16** as well as Man analog **21**, additional CSPs were observed for residues remote from the carbohydrate binding site (Figure S9). These residues, prominently featuring K257 and G259 in the short loop, were previously demonstrated to constitute an allosteric network involved in the regulation of Ca²⁺ recognition of Langerin¹. Hence, we hypothesize that this allosteric network might contribute to the recognition of glycans as well as glycomimetics².

While the CSP trajectories in the short loop were conserved between the Glc and the Man scaffold, residues associated with the carbohydrate binding site such as E285 and W252 displayed altered trajectories (Figure S9). This observation potentially results from conserved Ca²⁺-dependent interactions for both the Glc and Man scaffold which transduce allosteric effects. By contrast, changes in the chemical environment due to unique secondary interactions formed by e.g. **16** are locally constrained.

Supporting Figures

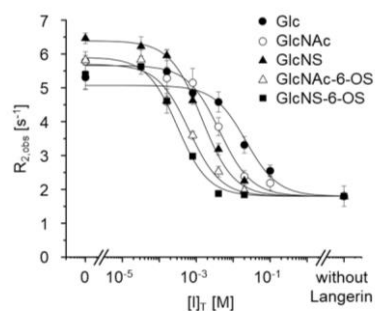


Figure S1. K_I determination for sulfated GlcNAc derivatives.

The K_I determination for heparin-derived GlcNAc derivatives *via* ^{19}F R_2 -filtered NMR revealed the impact of sulfation patterns on monosaccharide affinity. Obtained K_I values are given in Table S1.

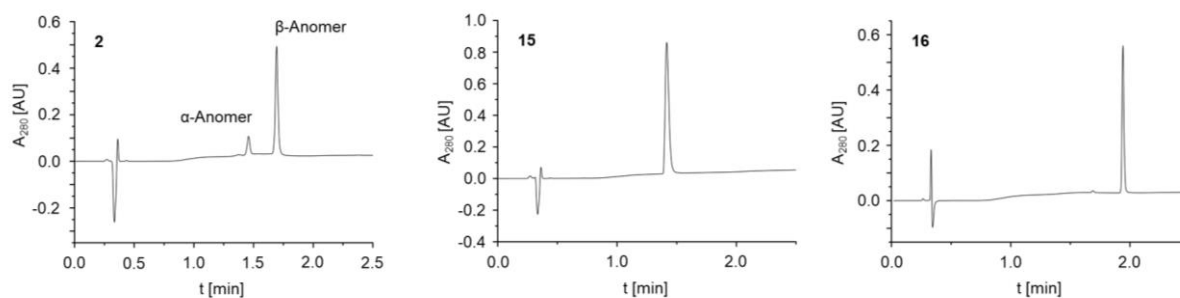


Figure S2. Analytical HPLC traces for GlcNS analogs **2**, **15** and **16**.

The purity of **2**, **15** and **16** was determined to be >95% using analytical reversed-phase HPLC (gradient: 3% to 30% acetonitrile in 0.1% TFA in H_2O in 2.5 min). The assignment of the two peaks for **2** to the α - and the β -anomer were validated via ^1H NMR and ESI MS.

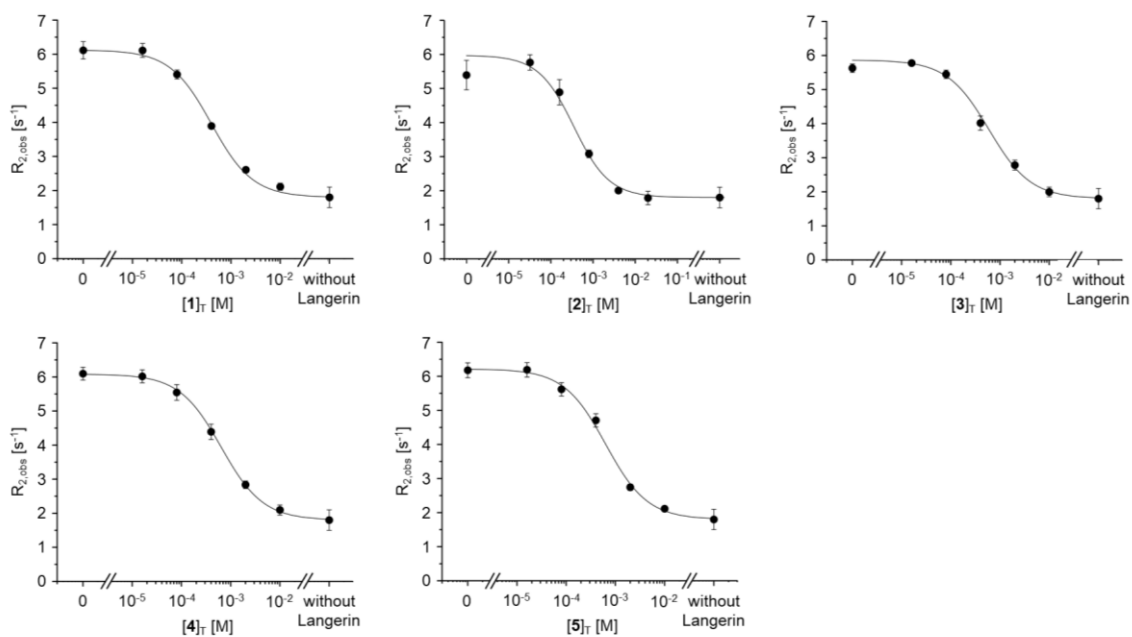


Figure S3. K_i determination for GlcNS analogs 1 to 5.

Competitive binding experiments served to determine the affinities for the GlcNS analog library. Obtained K_i values are given in Table S2.

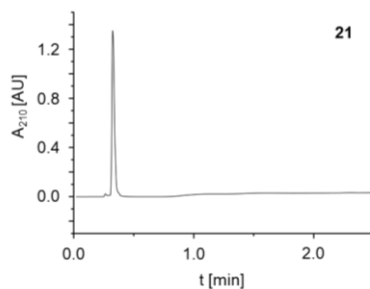


Figure S4. Analytical HPLC trace for Man analog 21.

The purity of **21** was determined to be >95% using analytical reversed-phase HPLC (gradient: 3% to 30% acetonitrile in 0.1% TFA in H_2O in 2.5 min).

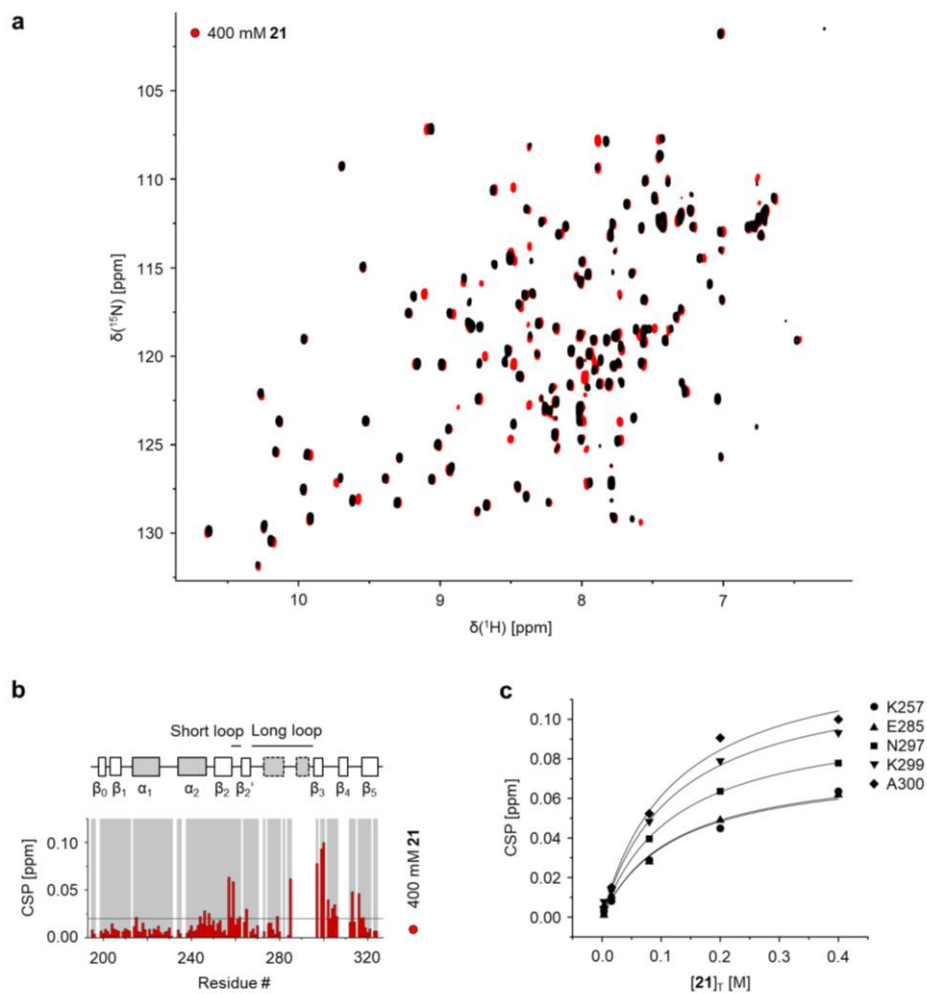


Figure S5. K_D determination for Man analog 21.

a and b. ^{15}N HSQC NMR experiments served to validate the obtained K_I value for 2. Assigned resonances detected in the reference spectrum are highlighted (grey). **c.** Assigned resonances displaying fast chemical exchange and CSPs larger than 0.06 ppm were selected for the determination of K_D values. The obtained K_D value is given in Table 1.

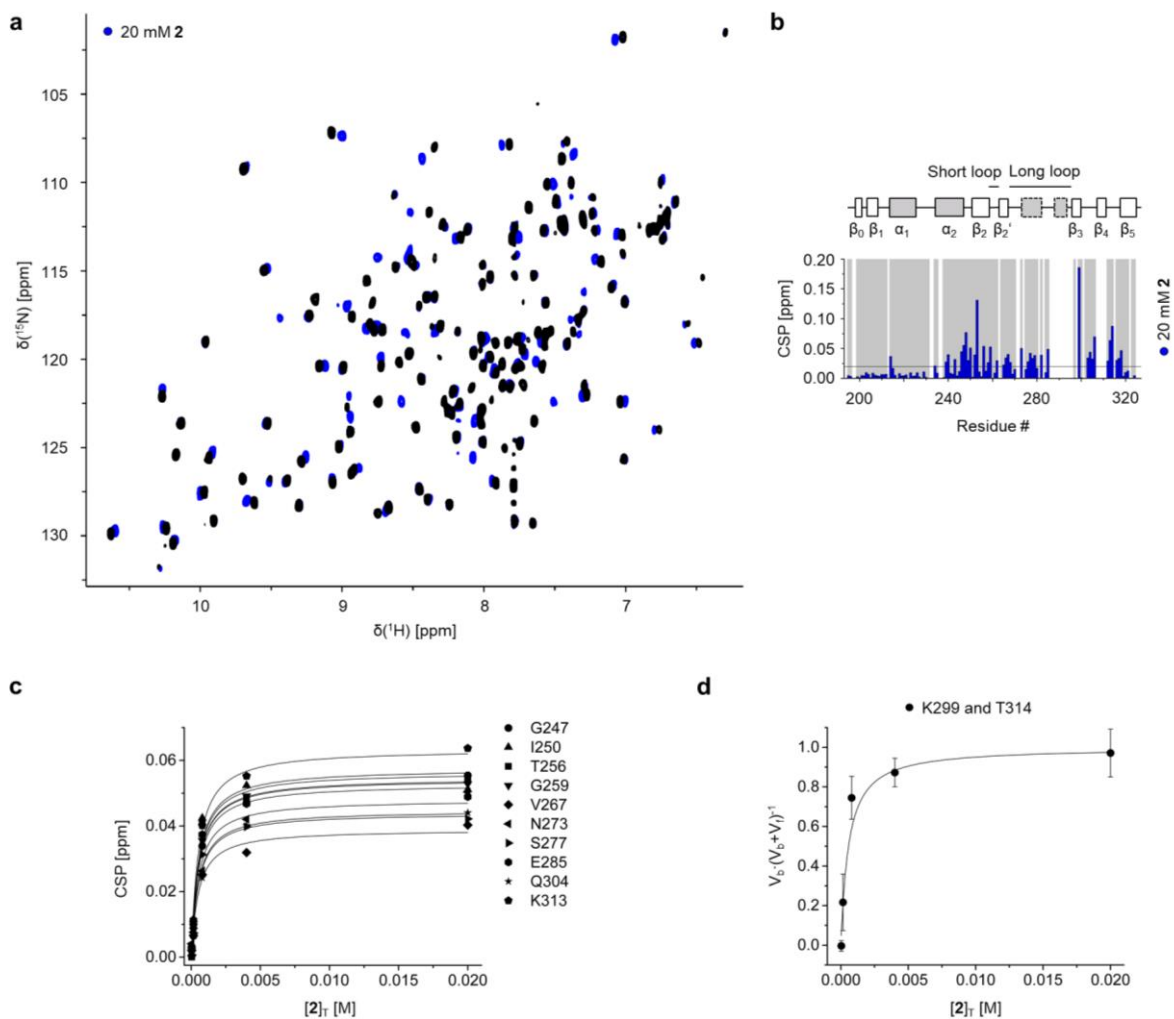


Figure S6. K_D determination for GlcNS analog **2.**

a and b. ^{15}N HSQC NMR experiments served to validate the obtained K_I value for **2**. Assigned resonances detected in the reference spectrum are highlighted (grey). **c.** Assigned resonances displaying fast chemical exchange and CSPs larger than 0.04 ppm were selected for the determination of K_D values. **d.** Additionally, a set of residues including K299 and T314 displayed slow exchange phenomena. For these residues, integrals V_f and V_b of resonances corresponding to the free and the bound state of the Langerin were utilized to determine K_D values. Obtained K_D values are given in Table 1.

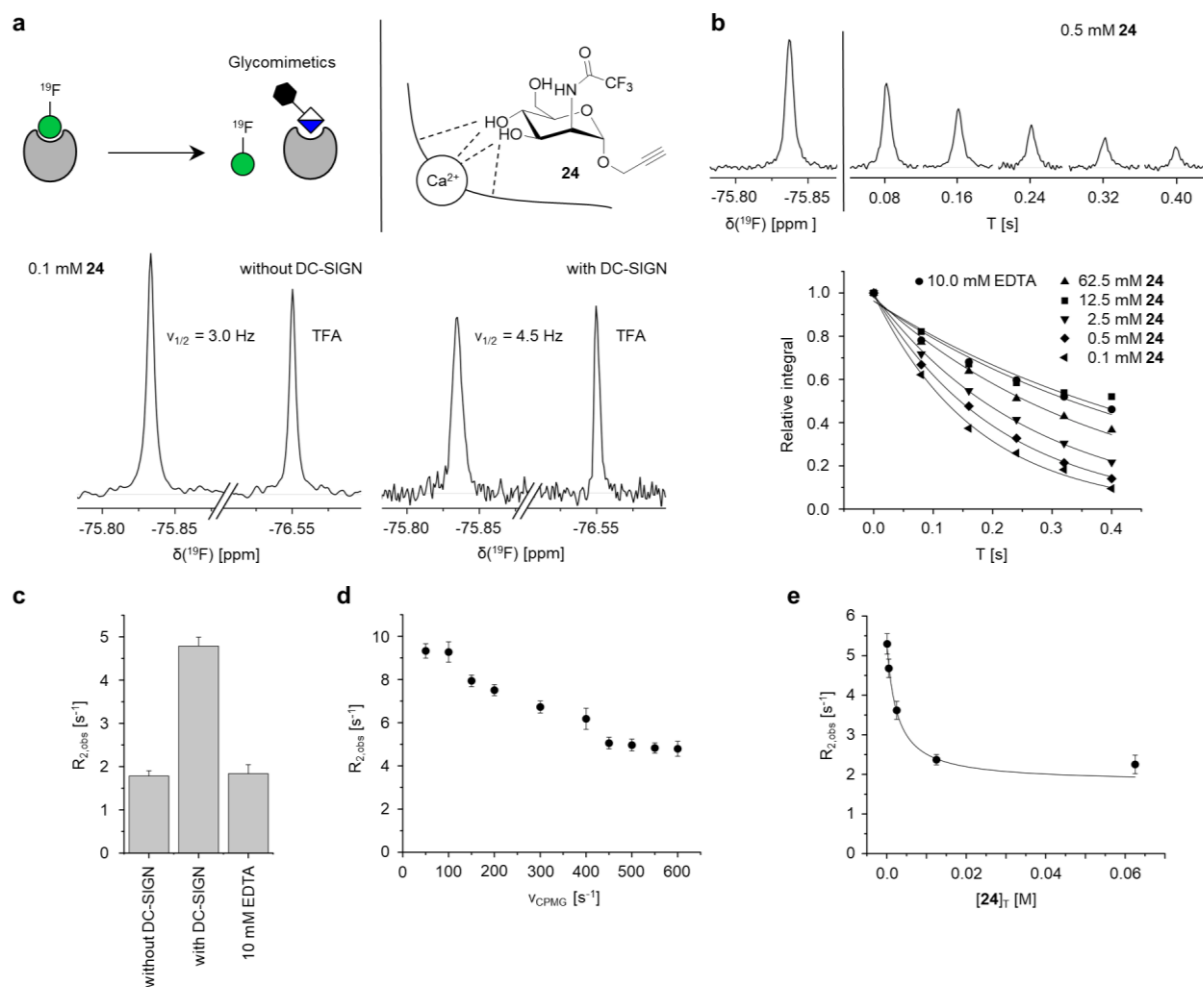


Figure S7. ^{19}F R_2 -filtered NMR assay development with DC-SIGN.

a. In presence of DC-SIGN, the ^{19}F NMR resonance of the trifluoroacetamido group of reporter ligand **24** displayed substantial line broadening. This phenomenon was utilized to develop the ^{19}F R_2 -filtered NMR reporter displacement assay following the procedure previously published for Langerin³. The spectrum in absence of DC-SIGN is processed with an exponential apodization function at 1.8 Hz. **b.** The interaction between **24** and DC-SIGN was quantified via the transversal relaxation rate $R_{2,\text{obs}}$ using the CPMG pulse sequence⁴⁻⁵. Representative decay curves in the presence of DC-SIGN are shown. **c.** The Ca^{2+} -dependency of the interaction was validated via addition of EDTA. The $R_{2,\text{obs}}$ value in absence of DC-SIGN was determined from four independent experiments. The standard error for the experiments in presence of DC-SIGN and EDTA is derived directly from the fitting procedure. **d.** Relaxation dispersion experiments for **24** in presence of DC-SIGN indicate a negligible exchange contribution $R_{2,\text{ex}}$ at a ν_{CPMG} value of 500 Hz. In contrast to Langerin, a considerable exchange contribution is observed at lower ν_{CPMG} values. **e.** A representative binding isotherm for the affinity determination for **24** is shown. The K_D value was determined from three independent titrations. The obtained K_D and additional parameters from the fitting procedure are given in Table S3.

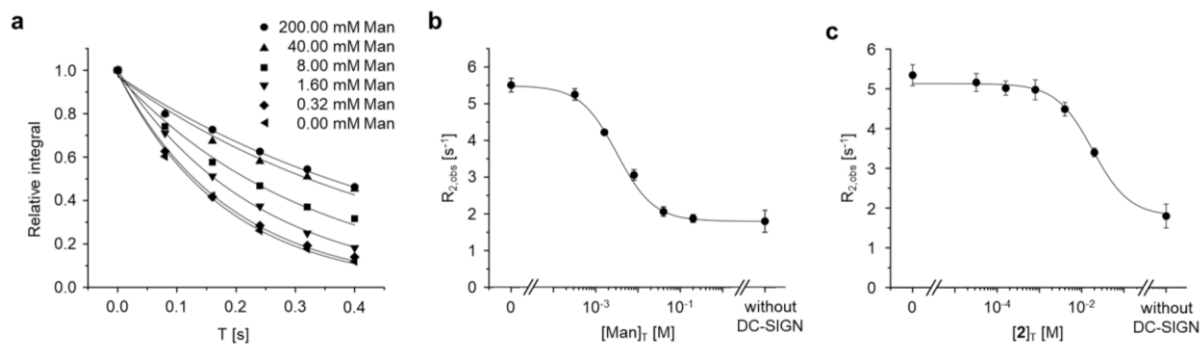


Figure S8. K_I determination for Man and GlcNS analog 2 with DC-SIGN.

a. Representative decay curves from the competitive binding experiments with Man are shown. **b and c.** Titration with Man revealed an affinity consistent with literature values while the K_I value determined for **2** indicated specificity against DC-SIGN⁶. Obtained K_I values are given in Table 1.

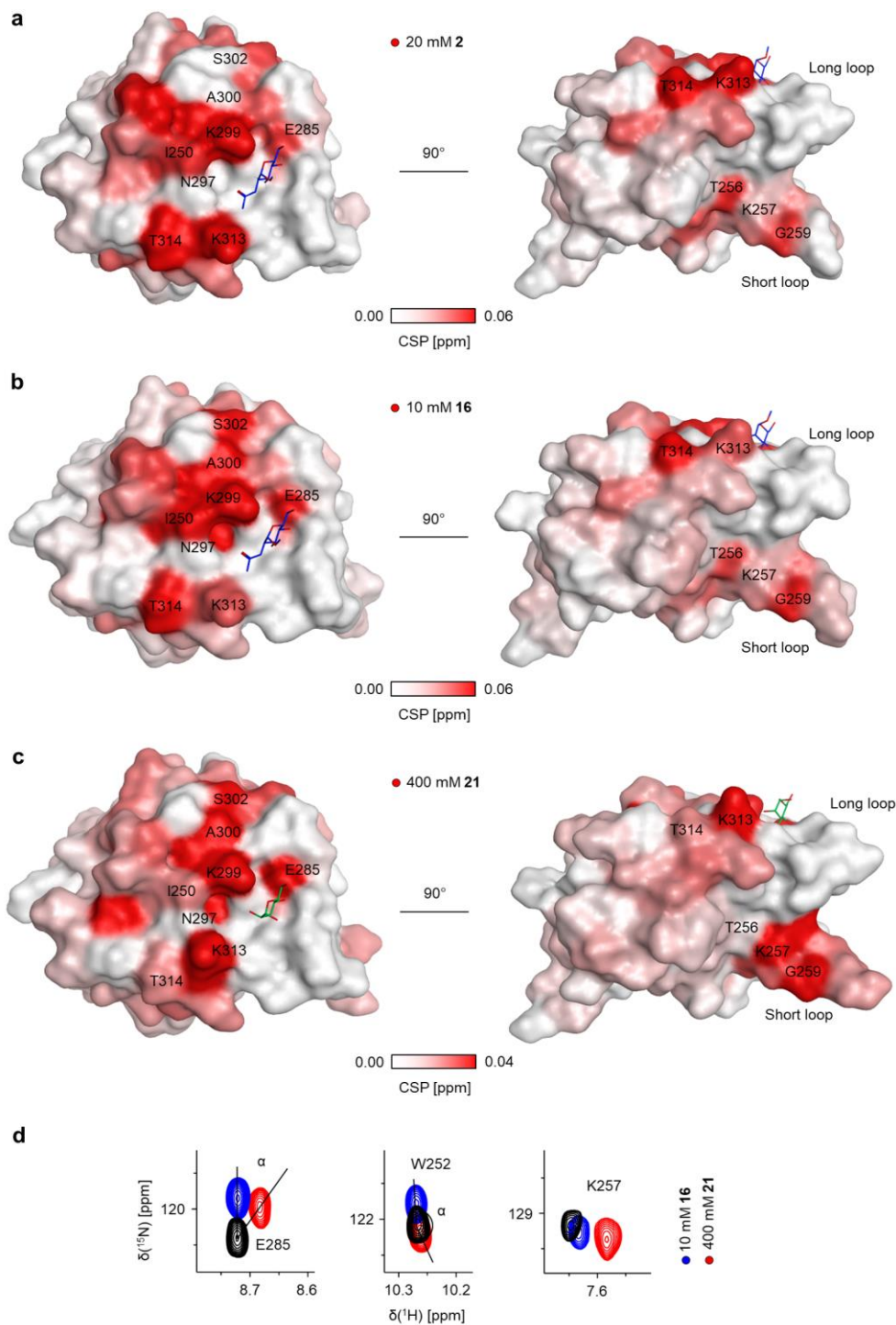


Figure S9. ^{15}N HSQC NMR binding mode analysis for GlcNS analogs **2, **16** and Man analog **21**.**

a to c. The mapping of CSP values on the X-ray structure of Langerin in complex with GlcNAc or Man (PDB code: 4N32 or 3P5F) validated a Ca^{2+} -dependent binding mode for **2** and **16** as indicated by CSPs observed for E285 and K299⁷⁻⁸. Additionally, CSPs were observed for N297, A300 and S302, residues also affected upon recognition of Man or **21**. By contrast, Y251 and I250 displayed considerably increased CSP values compared to **21**, while a relative decrease was observed for K313. This decrease was accompanied by a relative increase for the proximal T314. Notably, residues that display considerably increased CSP values can predominantly associated with F315 and N307 which were not assigned. This also hold true for W252 and W306 that displayed smaller relative increases. Accordingly, the observed CSP pattern might be induced by interactions formed between **2** or **16** and F315 rather than K313. Similar to Man and **21**, CSPs were also observed in remote regions of the C-type lectin-like domain fold, particularly for K257 and G259 in the short loop region. This might indicate a modulation of the previously reported allosteric network¹. **d.** A comparison of titrations with **16** and **21** revealed distinct CSP trajectories for residues associated with the carbohydrate binding site such as E285 or W252 while trajectories of residues located in remote regions of the C-type lectin-like fold such as K257 were conserved.

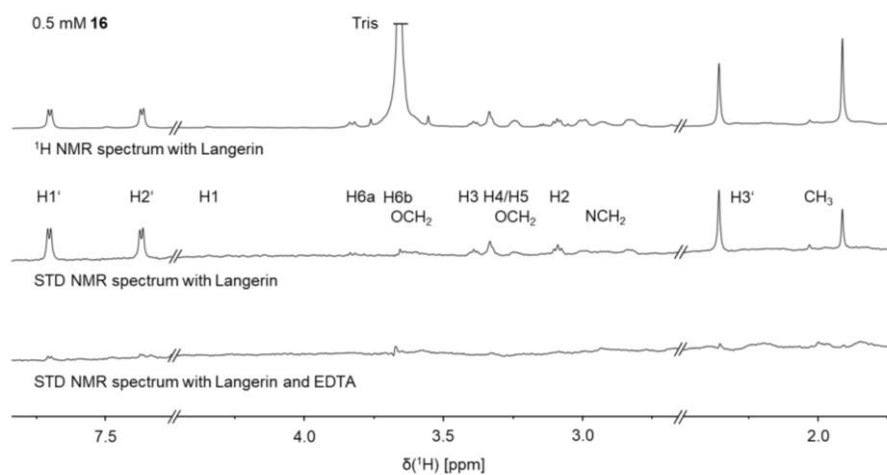


Figure S10. EDTA control experiment for GlcNS analog **16 by STD NMR spectroscopy.**

The abrogation of the STD effect after addition of 10 mM EDTA validated the Ca²⁺-dependent binding mode **16**. STD NMR spectra were recorded at saturation times t_{sat} of 2.0 s and are magnified 12-fold.

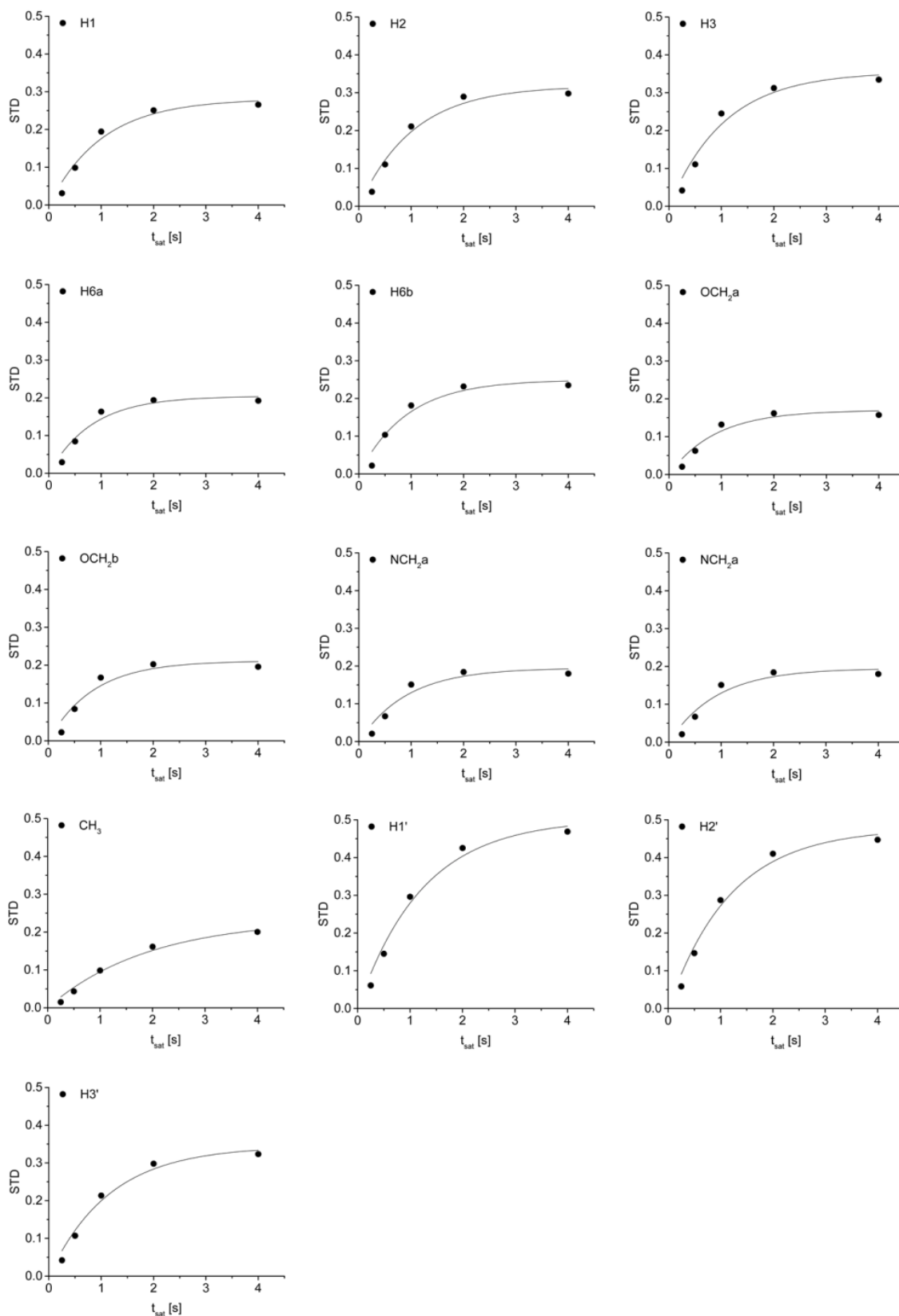


Figure S11. STD NMR build-up curves for GlcNS analog 16.

Equation 5 was fitted to STD values to calculate STD_0' values for the determination of the binding epitope of **16**.

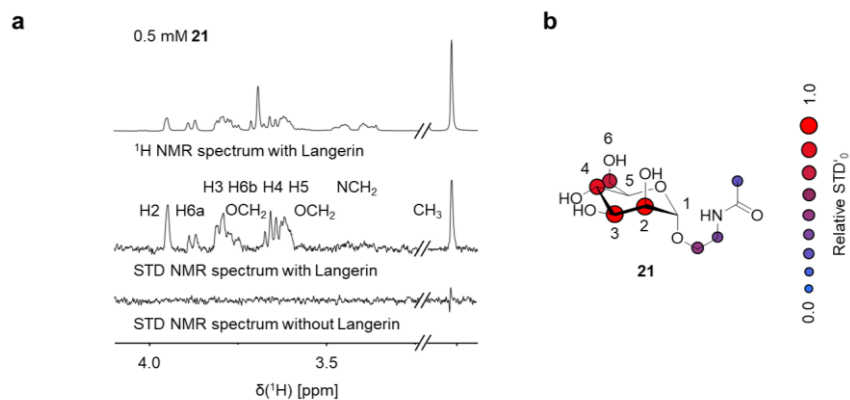


Figure S12. STD NMR epitope mapping for Man analog 21.

a. STD NMR experiments served to investigate the interaction of **21** with Langerin. STD NMR spectra were recorded at saturation times t_{sat} of 0.4 s and are magnified 8-fold. **b.** The epitope for **21** was determined from build-up curves and suggests a solvent exposed orientation for acetylated ethylamino linker (Figure S13).

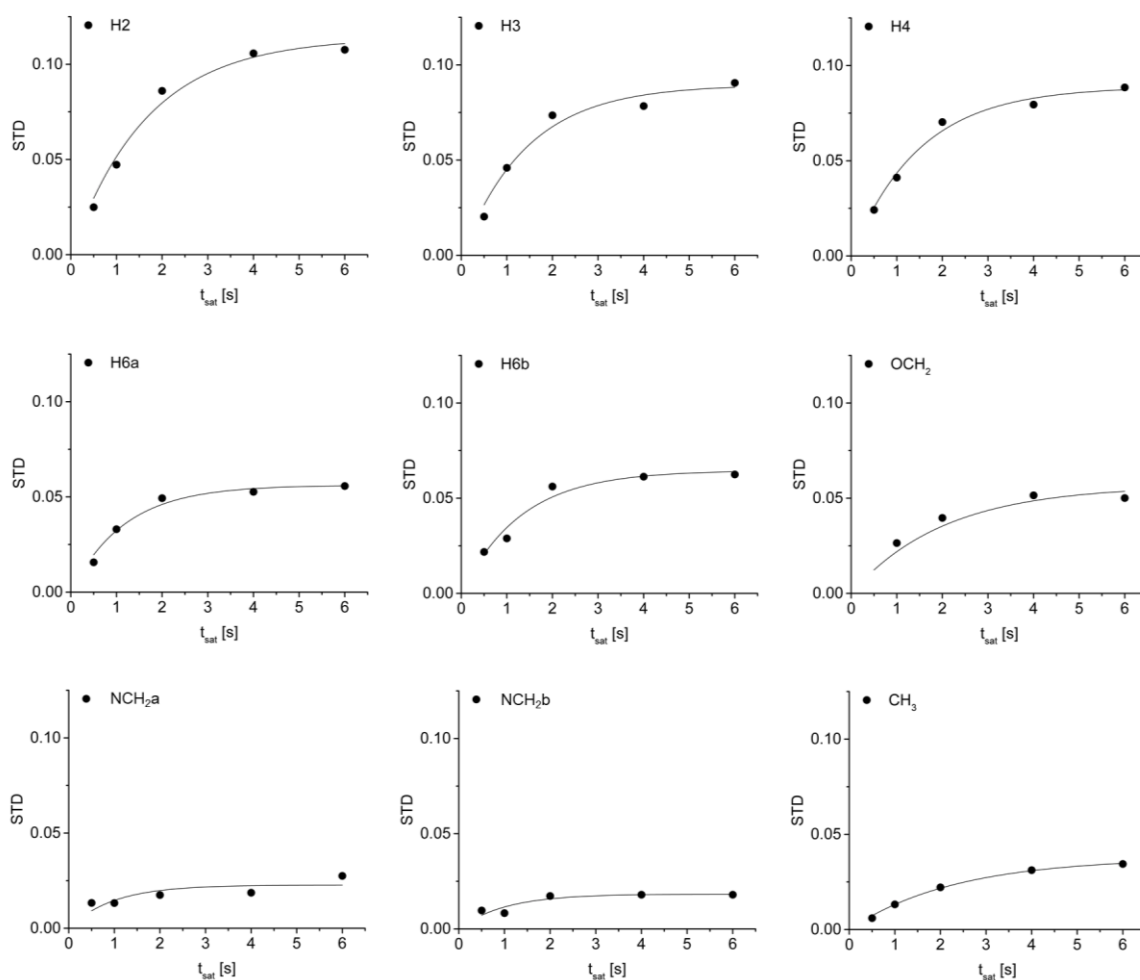


Figure S13. STD NMR build-up curves for Man analog 21.

Equation 5 was fitted to STD values to calculate STD_0^i values for the determination of the binding epitope of **21**.

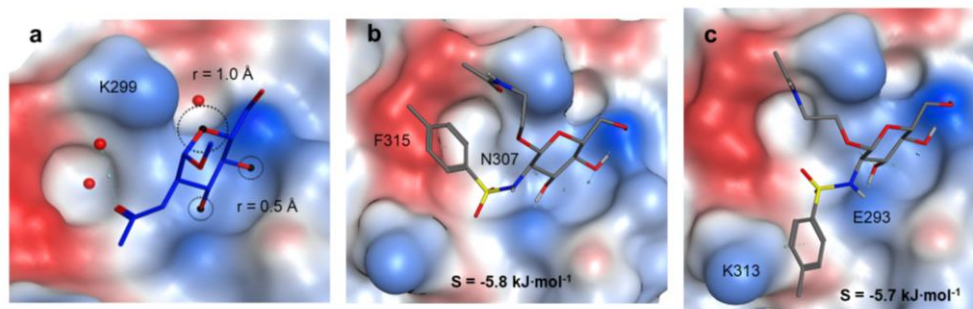


Figure S14. Molecular docking for GlcNS analog 16.

a. A pharmacophore model was defined to guide the initial placement of **16** in the carbohydrate binding site of Langerin (PDB code: 4N32) and to constrain the orientation of the Glc scaffold during the force field-based refinement of docking poses⁷. All features displayed require an oxygen atom within the indicated spheres. **b.** Four out of ten generated docking poses resemble the depicted conformation of **16**. The selected docking pose predicted the formation of π - π interactions between the phenyl ring and F315 as well as the formation of a hydrogen bond between the sulfonamide group and N307. The acetylated ethylamino linker displays high solvent exposure. Accordingly, this docking pose is consistent with both ¹⁵N HSQC and STD NMR experiments. **c.** The depicted alternative conformation of **16** is representative for three out of ten generated docking poses. The selected docking pose predicts the formation of cation- π interaction between the phenyl ring and K313 as well as the formation of a hydrogen bond between the sulfonamide and E293. The acetylated ethylamino linker displays high solvent exposure. However, this docking pose was less consistent with the ¹⁵N HSQC NMR results, particularly the relative decrease of CSP values for K313. The molecular docking study afforded three additional unique docking poses for **16** that were excluded due to unfavorable dihedral angles for the sulfonamide linker. The receptor surface is colored according to its lipophilicity (lipophilic: red, hydrophilic: blue).

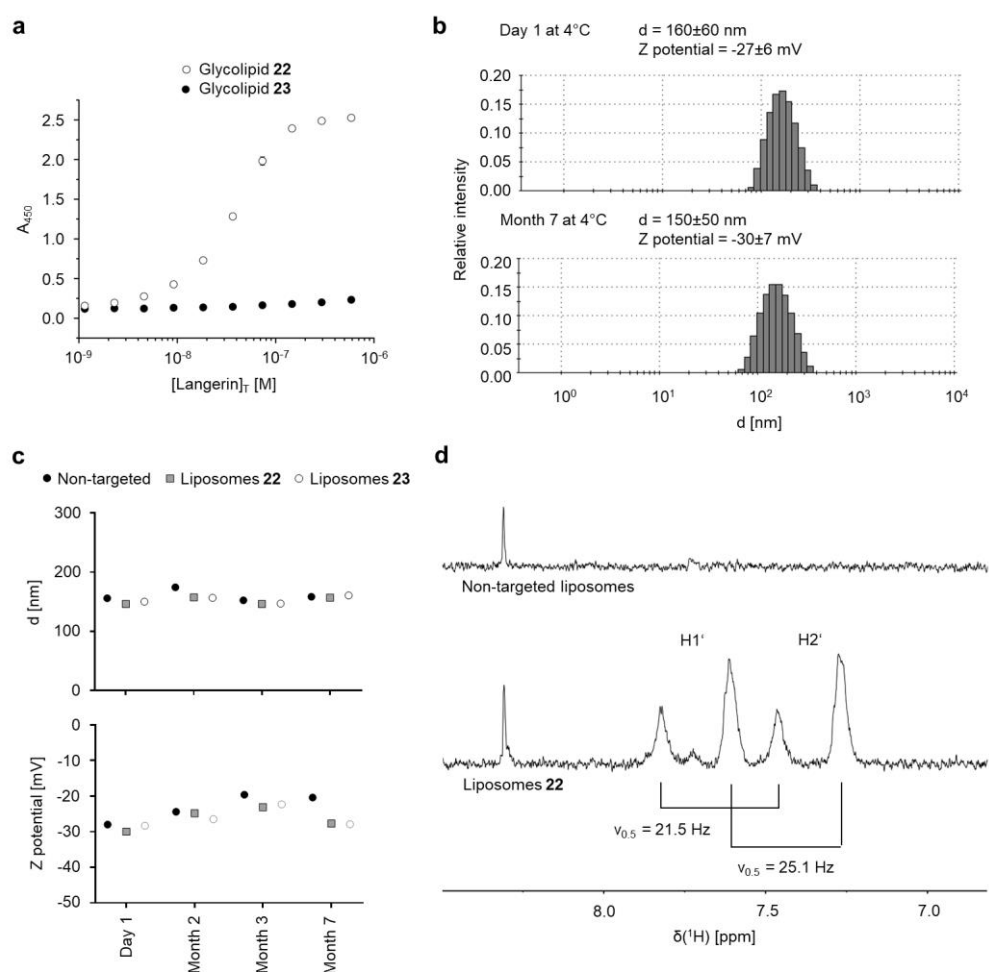


Figure S15. Characterization of liposomes 22 and 23.

a. Lipid-ELLA experiments served to evaluate the affinity of glycolipids **22** and **23** for the Langerin. No binding was detected for glycolipid **23**, bearing Man analog **21**. In contrast, glycolipid **22**, bearing GlcNS analog **16** displayed a dose-dependent response validating the expected affinity increase over reference molecule **21**. **b. and c.** Dispersity and stability of the prepared liposomes were analyzed via DLS and electrophoresis experiments. Representative histograms are depicted for liposomes **22**. The liposomes are monodisperse ($d = 160 \pm 60 \text{ nm}$) and stable ($Z \text{ potential} = -27 \pm 6 \text{ mV}$) for up to seven months when stored at 4°C in PBS. **d.** 1H NMR experiments with liposomes **22** revealed two states for **16** as observed for resonances corresponding to H1' and H2' of the phenyl ring. Both states display a linewidth $\nu_{0.5}$ smaller than 30 Hz, indicating accessibility and residual flexibility due to their presentation on extended PEG chains. The alternative state potentially corresponds to targeting ligands oriented towards the lumen of the liposomes.

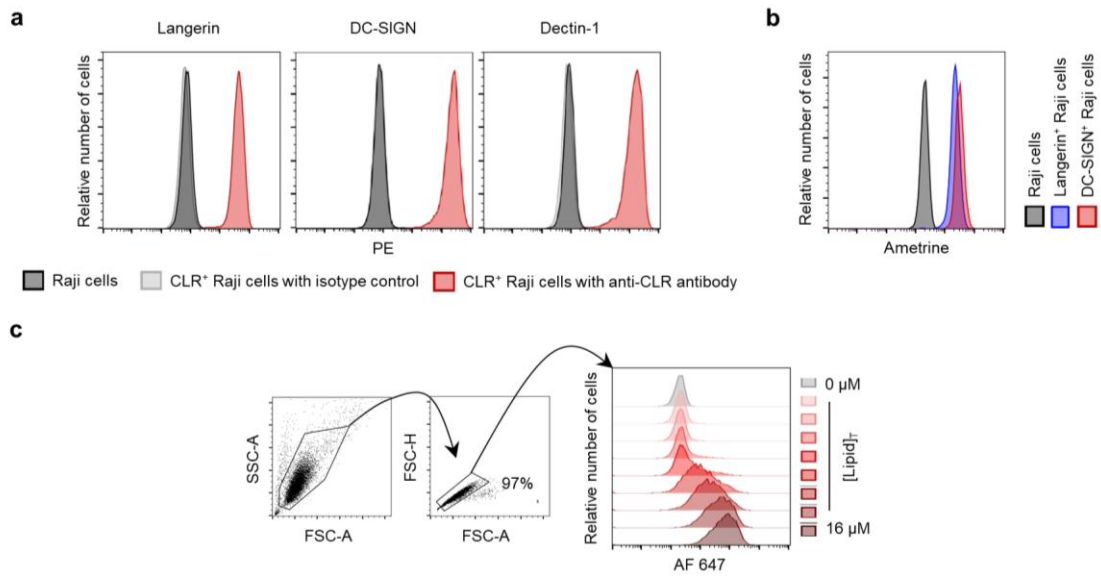


Figure S16. *In vitro* targeting of CLR⁺ Raji cells.

a. The expression of CLRs by the established Raji model cells was validated by flow cytometry using fluorophore-labeled anti-CLR antibodies. **b.** mRNA levels of for Langerin and DC-SIGN are comparable for the established Raji model cells as determined by flow cytometry analyzing Ametrine fluorescence. Ametrine is co-expressed with both CLRs on the same bicistronic vector used for transfection. **c.** The gating strategy and the corresponding histograms for dose-dependent internalization and binding of liposomes **22** to Langerin⁺ Raji cells at 4°C are exemplarily shown.

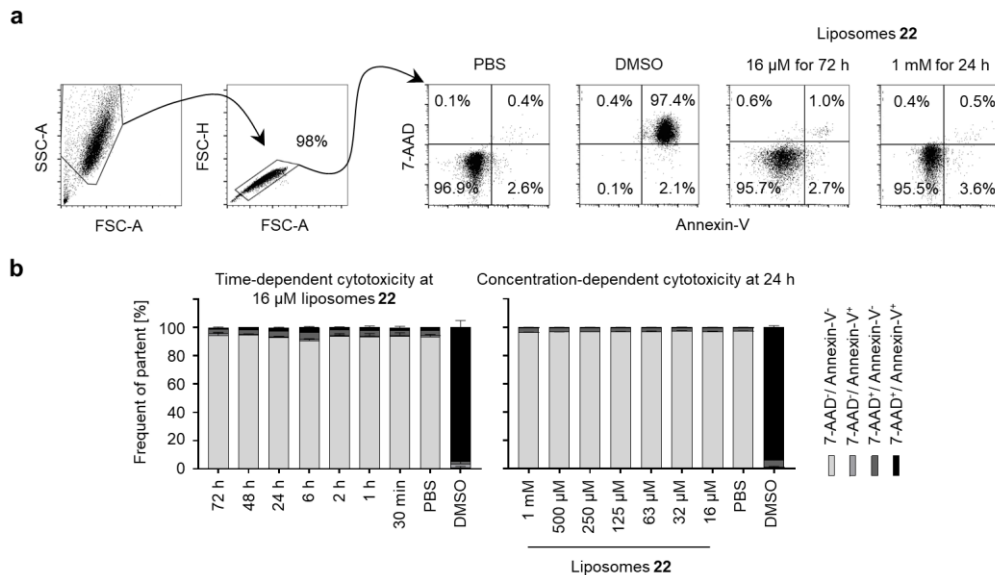


Figure S17. Induction of cytotoxicity by liposomes **22 with Langerin⁺ Raji cells.**

a. The gating strategy to evaluate the cytotoxicity of liposomes **22** is exemplarily shown for incubation of Langerin⁺ Raji cells with liposomes **22** at total lipid concentrations [Lipid]_T of 16 μM for 72 h and of 1 mM for 24 h. As a positive control, cells were exposed to 50% DMSO for 3 min following incubation for 72 h. **b.** Different incubation times and total lipid concentrations [Lipid]_T were analyzed. Staining with the early and late apoptotic markers Annexin-V and 7-AAD demonstrated negligible cytotoxicity of liposomes **22** even at high concentrations and long-term exposure.

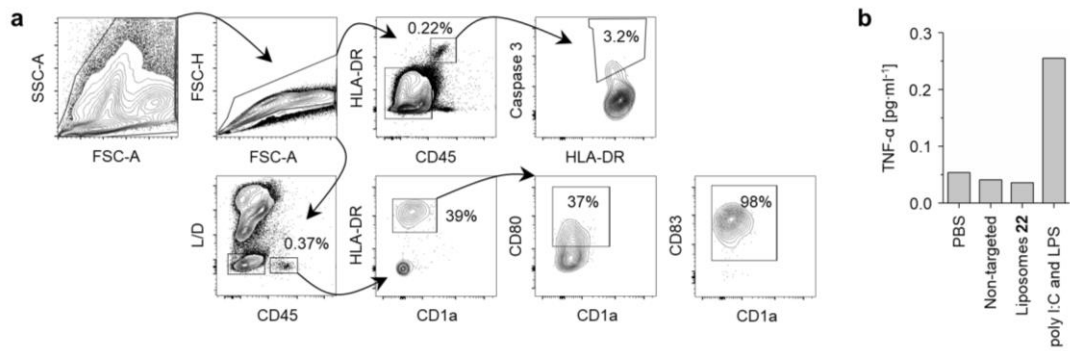
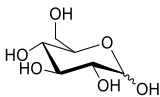
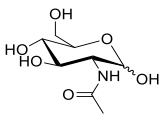
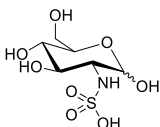
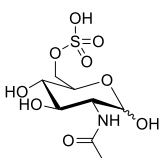
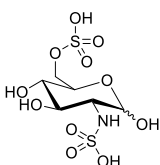


Figure S18. Induction of cytotoxicity and activation by liposomes 22 with LCs.

a. The gating strategy to evaluate the induction of cytotoxicity and activation by liposomes **22** with LCs is exemplarily shown after incubation at a total lipid concentration $[L]_T$ of 2.7 μ M for 48 h. Using epidermal cell suspension, LCs were identified as HLA-DR⁺-CD45⁺-CD1a^{high} cells with an additional viability gate to analyze their activation. Apoptosis was monitored by staining for active caspase 3. The activation of LCs was monitored via expression of CD80 and CD83. **b.** Additionally, the activation of LCs was analyzed by ELISA to monitor TNF- α secretion in one independent experiment. In contrast to the addition of poly I:C and LPS, liposomes **22** did not activate LCs.

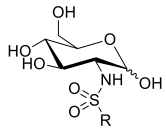
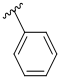
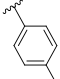
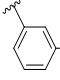
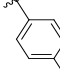
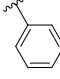
Supporting Tables

Table S1. Structure-activity relationship of sulfated GlcNAc derivatives.

Name	Structure	K _I [mM]	Relative potency ^a
Glc		21±4	0.20
GlcNAc		4.1±0.7	1.0
GlcNS		1.4±0.2	2.9
GlcNAc-6-OS		0.6±0.1	6.8
GlcNS-6-OS		0.28±0.06	14

^aThe relative potency was calculated utilizing the K_I value determined for GlcNAc.

Table S2. Structure-activity relationship of GlcNS analogs 1 to 5.

Name	Structure	R	K _I [mM]	Relative potency ^a
1			0.37±0.04	11
2			0.32±0.05	13
3			0.56±0.09	7.3
4			0.60±0.02	6.8
5			0.59±0.06	7.0

^a The relative potency was calculated utilizing the K_I value determined for GlcNAc.

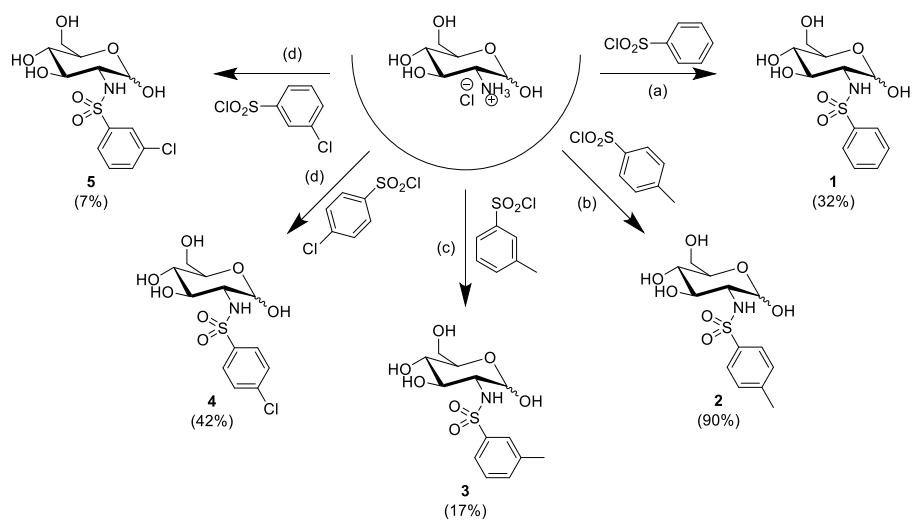
Table S3. ¹⁹F R₂-filtered NMR assay development with DC-SIGN.

Parameter	CRD
R _{2,f} [s ⁻¹]	1.8±0.3 ^a
R _{2,b} [s ⁻¹]	190±20 ^b
K _D [mM] for 24	2.3±0.5 ^b
K _I [mM] for Man	3.0±0.3

^a This value was determined from four independent experiments via ¹⁹F R₂-filtered NMR.

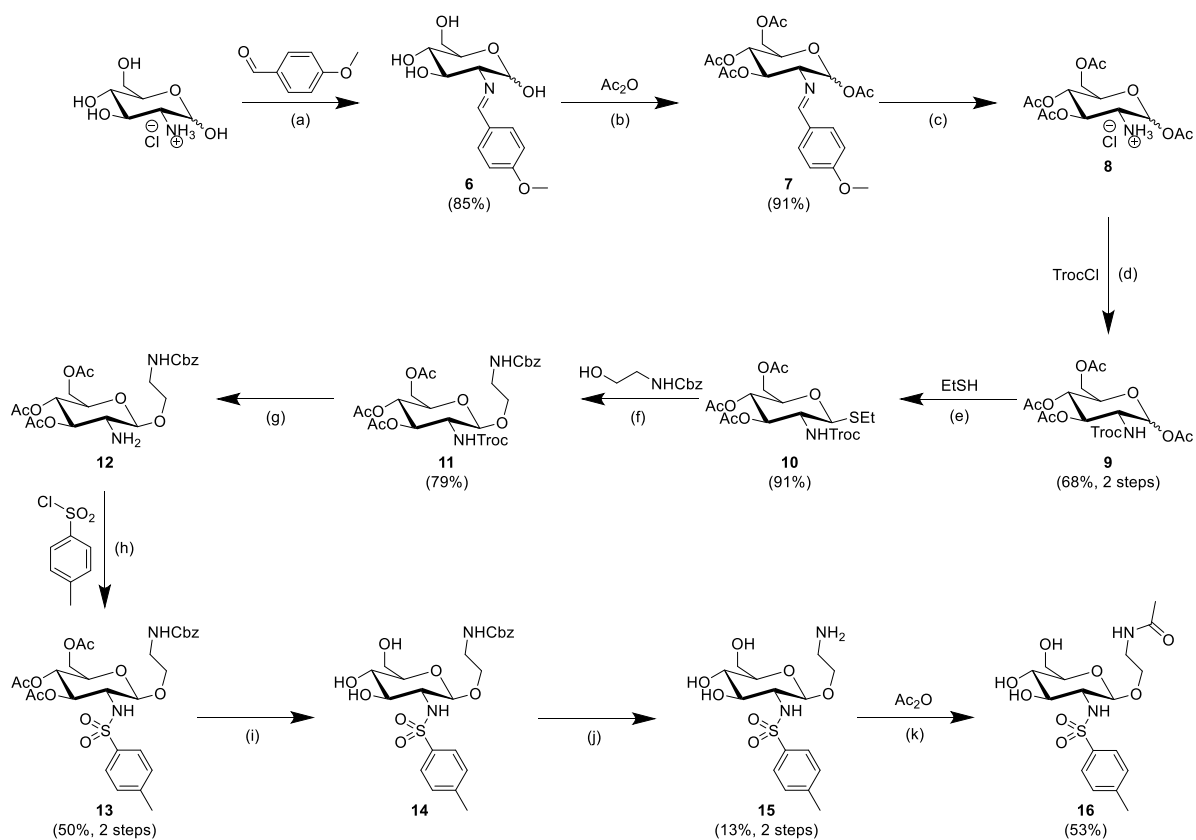
^b This value was determined from three independent titration experiments via ¹⁹F R₂-filtered NMR.

Supporting Schemes



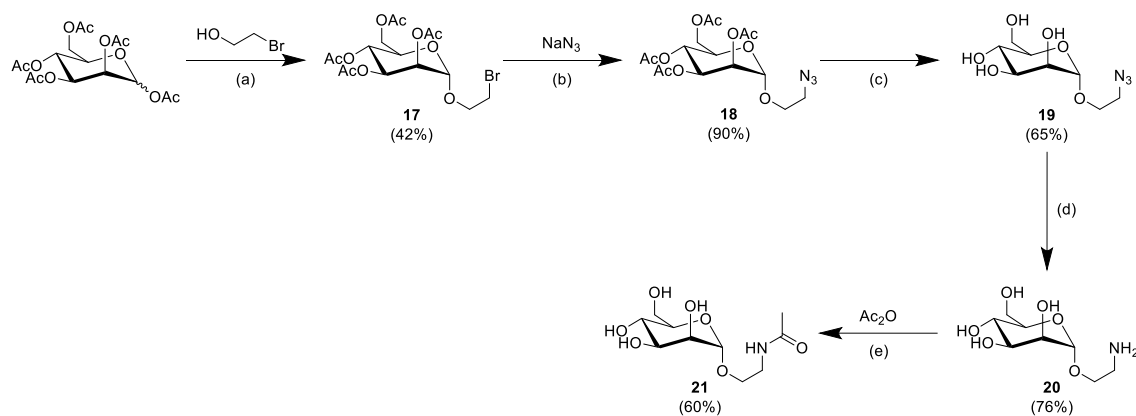
Scheme S1. Synthesis of GlcNS analogs 1 to 5.

Reaction conditions for the preparation of the library: (a) Et_3N , anhydrous MeOH, 0°C to room temperature; (b) acetone, room temperature; (c) DIPEA, DMSO, room temperature; (d) DIPEA, anhydrous MeOH, room temperature.



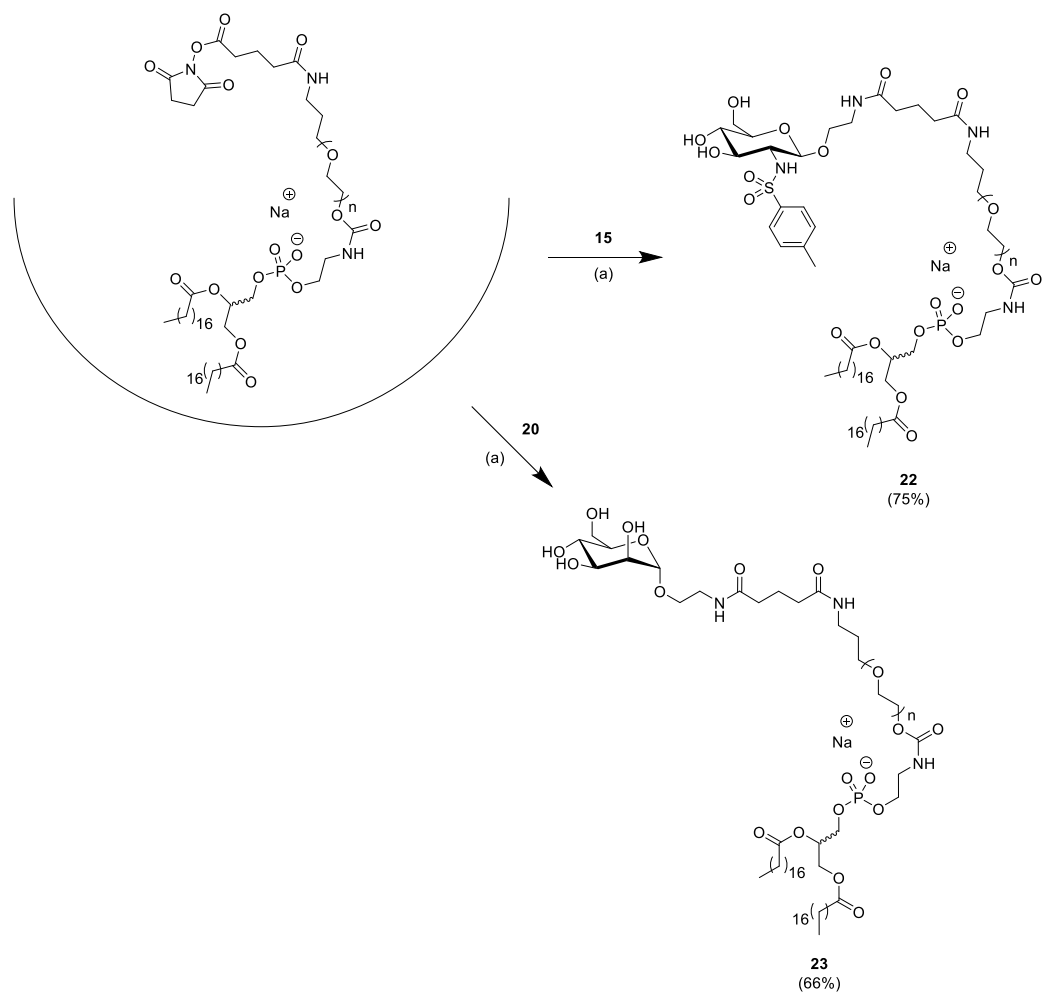
Scheme S2. Synthesis of GlcNS analogs 15 and 16.

Intermediate **10** was prepared as previously published⁹. Reaction conditions for the preparation of **16**: (a) 1 M aqueous NaOH, 0°C; (b) pyridine, 0°C to room temperature; (c) 5 M aqueous HCl, acetone, reflux; (d) pyridine, 0°C; (e) BF₃·OEt₂, anhydrous DCM, 0°C to room temperature; (f) DMTST, anhydrous DCM, room temperature; (g) Zn, AcOH, room temperature; (h) pyridine, room temperature; (i) MeONa, anhydrous MeOH, room temperature; (j) H₂, Pd/C, EtOH, room temperature; (k) MeOH, room temperature.



Scheme S3. Synthesis of Man analogs 20 and 21.

20 was prepared as previously published¹⁰. Reaction conditions for the preparation of **21**: (a) BF₃·OEt₂, anhydrous DCM, room temperature; (b) anhydrous DMF, 60°C; (c) MeONa, MeOH, room temperature; (d) H₂, Pd/C, anhydrous MeOH, room temperature; (e) MeOH, room temperature.



Scheme S4. Synthesis of glycolipids 22 and 23.

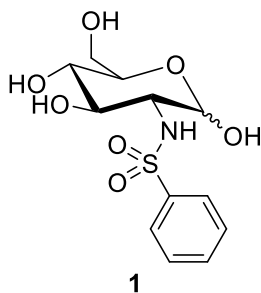
Reaction conditions for the preparation of **42** and **43**: (a) DMF:1M aqueous NaHCO₃ (1:10), pH 8.4, room temperature.

Methods

Synthetic Chemistry – Procedures

General remarks. Reagents and solvents used were purchased from Sigma Aldrich unless indicated otherwise and used as supplied without any further purification. Anhydrous solvents were taken from an anhydrous solvent system (JC-Meyer Solvent Systems). Column chromatography was carried out using silica gel at a pore size from 40 Å to 60 Å (Machery Nagel). Reversed-phase column chromatography was carried out using Chromabond endcapped C₁₈ columns at a pore size of 60 Å (Machery Nagel or Merck Millipore). Analytical TLC was performed on glass plates coated with silica gel at a pore size of 60 Å (Machery Nagel). Compounds were detected via 3-methoxyphenol reagent (0.2% 3-methoxyphenol in EtOH: 2 N sulfuric acid in EtOH (1:1)), ninhydrin reagent (1.5 g ninhydrin in 15 ml acetic acid and 500 ml MeOH) or CAM reagent (1.0 g Ce(SO₄)₂·4H₂O and 2.5 g ammonium molybdate pentahydrate in 96 ml of H₂O and 6 ml of concentrated H₂SO₄) upon heating or via UV adsorption ($\lambda = 254$ nm). NMR experiments were either conducted on a PremiumCompact 400 MHz or 600 MHz spectrometer (Agilent) and an Avance II 500 MHz or an Avance III 400 MHz spectrometer (Bruker). Chemical shifts were referenced to the internal standards CHCl₃ ($\delta(^1\text{H}) = 7.26$ ppm and $\delta(^{13}\text{C}) = 77.1$ ppm), H₂O ($\delta(^1\text{H}) = 7.26$ ppm), MeOH ($\delta(^1\text{H}) = 4.87$ ppm, $\delta(^{13}\text{C}) = 49.0$ ppm). Coupling constants are reported in Hz and coupling patterns are indicated as s for singlet, d for doublets, dd for doublets of doublets, ddd for doublets of doublets of doublets, t for triplets, dt for doublets of triplets, td for triplet of doublets, q for quartets and m for multiplets. Signals were assigned by means of COSY, TOCSY, ¹³C HSQC and H2BC NMR experiments¹¹. Stereoselectivity at the anomeric position of the mannose and the glucosamine scaffold was analyzed by measuring ¹J_{C1,H1} coupling constants¹². NMR spectra were processed with MestReNova¹³. ESI-MS analysis was conducted using an 1100 Series LC/MS coupled to a G1946D ESI-Q spectrometer (Agilent). HR ESI-MS analysis was conducted using an Acquity H-Class UPLC/MS coupled to a Xevo G2-S ESI-Q-TOF spectrometer (Waters). Preparative HPLC was performed on a 1100 Series LC/MS (Thermo Scientific) using a preparative Nucleodur C18 column (Machery Nagel). Analytical HPLC was performed on an Acquity UPLC system using an analytical BEH C18 column (Waters).

2-deoxy-2-phenylsulfonylamido-D-glucopyranose



Glucosamine hydrochloride (50 mg, 232 μmol) was dissolved in anhydrous MeOH (2.3 ml) via the addition of Et_3N (81 μl , 580 μmol). Benzenesulfonyl chloride (178 μl , 1.39 mmol) was added dropwise at 0°C under argon atmosphere. The reaction was allowed to heat up to room temperature and stirred for 2 h. More Et_3N (32 μl , 230 μmol) and benzenesulfonyl chloride (89 μl , 695 μmol) were added dropwise at 0°C . The reaction was again allowed to heat up to room temperature and stirred for another 2h. Solvents were evaporated *in vacuo* and the residue was purified via reversed-phase column chromatography (gradient: H_2O , 1%, 5% MeOH in H_2O and elution with 10% MeOH in H_2O) and subsequently via column chromatography (gradient: DCM, 5% MeOH, 10% MeOH in DCM and elution with 20% MeOH in DCM). Silica particles were removed via filtration in MeOH with a cellulose acetate membrane at a pore size 0.2 μm to yield to yield an α/β -mixture of **1** (23.9 mg, 75 μmol , 32%) as a white solid.

The ratio of α - and β -anomer was determined to be 5:1 via ^1H NMR. Here, only chemical shifts corresponding to the β -anomer are documented. As a result of the low signal intensities for the α -anomer the corresponding resonances were not assigned.

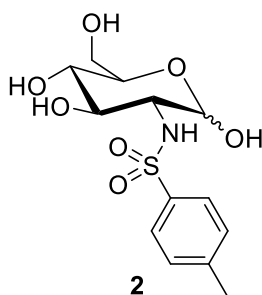
^1H NMR (400.0 MHz, MeOD, β -anomer): δ = 7.96 – 7.87 ppm, m, 2 H (aromatic H); δ = 7.64 – 7.45 ppm, m, 3 H (aromatic H); δ = 4.78 ppm, d, 1 H, J = 3.5 Hz (H1); δ = 3.76 – 3.68 ppm, m, 2 H (H6a, H5); δ = 3.69 – 3.55 ppm, m, 2 H (H6a, H3); δ = 3.30 – 3.24 ppm, m, 1 H (H4); δ = 3.13 ppm, dd, 1 H, J = 10.1, 3.5 Hz (H2).

^{13}C NMR (100.6 MHz, MeOD, β -anomer): δ = 143.4 ppm, 1 C (aromatic C); δ = 133.4 ppm, 1 C (aromatic C); δ = 130.0 ppm, 2 C (aromatic C); δ = 128.0 ppm, 2 C (aromatic C); δ = 92.9 ppm, 1 C (C1); δ = 72.8 ppm, 1 C (C5); δ = 72.5 ppm, 1 C (C3); δ = 72.2 ppm, 1 C (C4); δ = 62.6 ppm, 1 C (C6); δ = 59.9 ppm, 1 C (C2).

R_f = 0.50 with 20% MeOH in DCM.

HR ESI-MS for $\text{C}_{12}\text{H}_{17}\text{NO}_7\text{S}$: $m\cdot z^{-1}(\text{M}+\text{Na}^+)_{\text{calc}} = 342.062$; $m\cdot z^{-1}(\text{M}+\text{Na}^+)_{\text{obs}} = 342.063$.

2-deoxy-2-N-tosyl-D-glucopyranose



Glucosamine hydrochloride (3.0 g, 13.9 mmol) were dissolved in acetone (15 ml). Tosyl chloride (2.6 g, 13.9 mmol) was added and reaction was stirred for 4 h at room temperature. Solvents were removed *in vacuo* and the residue was purified via flash chromatography (15% MeOH in DCM) to yield an α/β -mixture of **2** (4.1 g, 12.5 mmol, 90%) as a white solid.

The ratio of α - and β -anomer was determined to be 10:1 via ^1H NMR. Here, only chemical shifts corresponding to the β -anomer are documented. As a result of the low signal intensities for the α -anomer the corresponding resonances were not assigned.

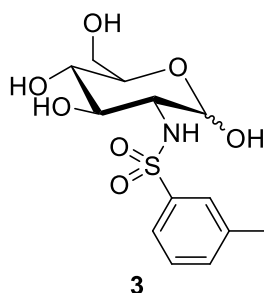
^1H NMR (400.0 MHz, MeOD, β -anomer): δ = 7.82 – 7.77 ppm, m, 2 H (aromatic H); δ = 7.37 – 7.32 ppm, m, 2 H (aromatic H); δ = 4.77 ppm, d, 1 H, J = 3.5 Hz (H1); δ = 3.76 – 3.69 ppm, m, 2 H (H6a, H5); δ = 3.68 – 3.55 ppm, m, 2 H (H6a, H3); δ = 3.30 – 3.24 ppm, m, 1 H (H4); δ = 3.09 ppm, dd, 1 H, J = 10.1, 3.6 Hz (H2); δ = 2.41 ppm, s, 3 H (CH₃).

^{13}C NMR (100.6 MHz, MeOD, β -anomer): δ = 144.4 ppm, 1 C (aromatic C); δ = 140.4 ppm, 1 C (aromatic C); δ = 130.6 ppm, 2 C (aromatic C); δ = 128.1 ppm, 2 C (aromatic C); δ = 92.9 ppm, 1 C (C1); δ = 72.8 ppm, 1 C (C5); δ = 72.5 ppm, 1 C (C3); δ = 72.2 ppm, 1 C (C4); δ = 62.6 ppm, 1 C (C6); δ = 59.8 ppm, 1 C (C2); δ = 21.5 ppm, 1 C (CH₃).

R_f = 0.38 with 10% MeOH in DCM.

HR ESI-MS for C₁₃H₁₉NO₇S: $m\cdot z^{-1}(\text{M}+\text{Na}^+)_{\text{calc}}$ = 356.078; $m\cdot z^{-1}(\text{M}+\text{Na}^+)_{\text{obs}}$ = 356.077.

2-deoxy-2-3'-(methyl)phenylsulfonlamido-D-glucopyranose



Glucosamine hydrochloride (49 mg, 227 μmol) was dissolved in DMSO (4.6 ml) via addition of DIPEA (240 μl , 1.39 mmol). Next, 3-methylphenylsulfonyl chloride (84 μl , 580 μmol) was slowly added and the reaction mixture was stirred for 2 h at room temperature. The reaction was quenched with MeOH and solvents were removed *in vacuo*. Residual DMSO was removed via lyophilization. The residue was purified via column chromatography (gradient: DCM, 5% MeOH in DCM and elution with 10% MeOH in DCM) and reversed-phase column chromatography (gradient: H₂O, 1%, 5% MeOH in H₂O and elution with 10% MeOH in H₂O) to yield **3** (12.9 mg, 39 μmol , 17%) as a white solid after lyophilization.

The ratio of α - and β -anomer was determined to be 10:1 via ¹H NMR. Here, only chemical shifts corresponding to the β -anomer are documented. As a result of the low signal intensities for the α -anomer the corresponding resonances were not assigned.

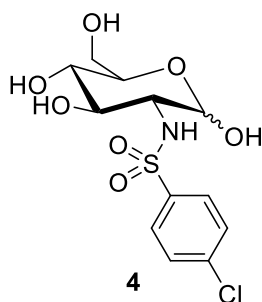
¹H NMR (400.0 MHz, MeOD, β -anomer): δ = 7.78 – 7.66 ppm, m, 2 H (aromatic H); δ = 7.45 – 7.38 ppm, m, 2 H (aromatic H); δ = 4.78 ppm, d, 1 H, J = 3.6 Hz (H1); δ = 3.76 – 3.68 ppm, m, 2 H (H6a, H5); δ = 3.68 – 3.56 ppm, m, 2 H (H6a, H3); δ = 3.30 – 3.24 ppm, m, 1 H (H4); δ = 3.12 ppm, dd, 1 H, J = 10.5, 3.6 Hz (H2); δ = 2.42 ppm, s, 3 H (CH₃).

¹³C NMR (100.6 MHz, MeOD, β -anomer): δ = 143.2 ppm, 1 C (aromatic C); δ = 140.4 ppm, 1 C (aromatic C); δ = 134.1 ppm, 1 C (aromatic C); δ = 129.9 ppm, 1 C (aromatic C); δ = 128.3 ppm, 1 C (aromatic C); δ = 125.1 ppm, 1 C (aromatic C); δ = 92.9 ppm, 1 C (C1); δ = 72.8 ppm, 1 C (C5); δ = 72.6 ppm, 1 C (C3); δ = 72.2 ppm, 1 C (C4); δ = 62.7 ppm, 1 C (C6); δ = 59.9 ppm, 1 C (C2); δ = 21.3 ppm, 1 C (CH₃).

R_f = 0.34 with 10% MeOH in DCM.

HR ESI-MS for C₁₂H₁₉NO₇S: $m \cdot z^{-1}(M+Na^+)_{\text{calc}} = 356.078$; $m \cdot z^{-1}(M+Na^+)_{\text{obs}} = 356.079$.

2-deoxy-2-4'-(chloro)phenylsulfonylamido-D-glucopyranose



Glucosamine hydrochloride (51 mg, 234 μ mol) was dissolved in anhydrous MeOH (2.3 ml) via the addition of DIPEA (240 μ l, 1.39 mmol). 4-chlorophenylsulfonyl chloride (196 mg, 928 μ mol) was dissolved in anhydrous MeOH (1.0 ml) and slowly added. The reaction mixture was stirred 4 h at room temperature. Solvents were removed *in vacuo* and the residue was purified via reversed-phase column chromatography (gradient: H₂O, 1% MeOH in H₂O and elution with 5% MeOH in H₂O) to yield **4** (35 mg, 99 μ mol, 42%) as a white solid after lyophilization.

The ratio of α - and β -anomer was determined to be 4:1 via ¹H NMR. Here, only chemical shifts corresponding to the β -anomer are documented. As a result of the low signal intensities for the α -anomer the corresponding resonances were not assigned.

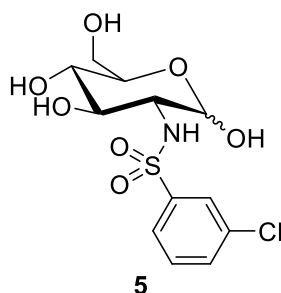
¹H NMR (400.0 MHz, MeOD, β -anomer): δ = 7.92 – 7.87 ppm, m, 2 H (aromatic H); δ = 7.56 – 7.51 ppm, m, 2 H (aromatic H); δ = 4.86 ppm, d, 1 H, *J* = 3.6 Hz (H1); δ = 3.77 – 3.69 ppm, m, 2 H (H6a, H5); δ = 3.68 – 3.55 ppm, m, 2 H (H6a, H3); δ = 3.29 – 3.23 ppm, m, 1 H (H4); δ = 3.14 ppm, dd, 1 H, *J* = 10.2, 3.5 Hz (H2).

¹³C NMR (100.6 MHz, MeOD, β -anomer): δ = 142.3 ppm, 1 C (aromatic C); δ = 139.4 ppm, 1 C (aromatic C); δ = 130.1 ppm, 2 C (aromatic C); δ = 129.8 ppm, 2 C (aromatic C); δ = 93.2 ppm, 1 C (C1); δ = 72.8 ppm, 1 C (C5); δ = 72.5 ppm, 1 C (C3); δ = 72.3 ppm, 1 C (C4); δ = 62.6 ppm, 1 C (C6); δ = 59.9 ppm, 1 C (C2).

R_f = 0.30 with 10% MeOH in DCM.

HR ESI-MS for C₁₂H₁₆ClNO₇S: $m \cdot z^{-1}(M+Na^+)_{\text{calc}} = 376.023$; $m \cdot z^{-1}(M+Na^+)_{\text{obs}} = 376.024$.

2-deoxy-2-3'-(chloro)phenylsulfonylamido-D-glucopyranose



Glucosamine hydrochloride (50 mg, 234 μ mol) was dissolved in anhydrous MeOH (2.3 ml) via addition of DIPEA (240 μ l, 1.39 mmol). 3-chlorophenylsulfonyl chloride (130 μ l, 930 μ mol) was slowly added and the reaction mixture was stirred for 4 h at room temperature. Solvents were removed *in vacuo* and the residue was purified via reversed-phase column chromatography (gradient: H₂O, 1% MeOH in H₂O and elution with 5% MeOH in H₂O) to yield **5** (6.0 mg, 17 μ mol, 7%) as a white solid after lyophilization.

The ratio of α - and β -anomer was determined to be 8:1 via ¹H NMR. Here, only chemical shifts corresponding to the β -anomer are documented. As a result of the low signal intensities for the α -anomer the corresponding resonances were not assigned.

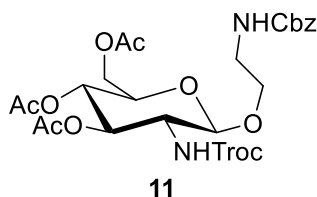
¹H NMR (400.0 MHz, MeOD, β -anomer): δ = 7.97 – 7.79 ppm, m, 2 H (aromatic H); δ = 7.63 – 7.47 ppm, m, 2 H (aromatic H); δ = 4.87 ppm, m, 1 H (H1); δ = 3.78 – 3.69 ppm, m, 2 H (H6a, H5); δ = 3.69 – 3.55 ppm, m, 2 H (H6a, H3); δ = 3.30 – 3.24 ppm, m, 1 H (H4); δ = 3.12 ppm, dd, 1 H, J = 10.6, 3.5 Hz (H2).

¹³C NMR (100.6 MHz, MeOD, β -anomer): δ = 145.5 ppm, 1 C (aromatic C); δ = 135.8 ppm, 1 C (aromatic C); δ = 133.2 ppm, 1 C (aromatic C); δ = 131.6 ppm, 1 C (aromatic C); δ = 128.0 ppm, 1 C (aromatic C); δ = 126.4 ppm, 1 C (aromatic C); δ = 93.2 ppm, 1 C (C1); δ = 72.8 ppm, 1 C (C5); δ = 72.5 ppm, 1 C (C3); δ = 72.3 ppm, 1 C (C4); δ = 62.6 ppm, 1 C (C6); δ = 60.0 ppm, 1 C (C2).

R_f = 0.51 with 10% MeOH in DCM.

HR ESI-MS for C₁₂H₁₆ClNO₇S: m·z⁻¹(M+Na⁺)_{calc} = 376.023; m·z⁻¹(M+Na⁺)_{obs} = 376.024.

(N-(Benzyloxycarbonyl)-2-aminoethyl)-2-deoxy-2-N-(2,2,2-trichloroethyloxy-carbonyl)-3,4,6-tri-O-acetyl- β -D-glucopyranoside



Intermediate **10** was prepared as previously published⁹. **10** (1.0 g, 1.0 mmol) and benzyl 2-hydroxyethylcarbamate (0.60 g, 3.1 mmol) were dissolved in DCM (40 ml) and stirred for 45 min at room temperature. DMTST (1.0 g, 3.8 mmol) was added and the reaction mixture was stirred overnight at room temperature. Solvents were removed *in vacuo* and the residue was purified via flash column chromatography (cyclohexane:EtOAc (1:1)) to yield **11** as a white solid (1.0 g, 1.4 mmol, 79%).

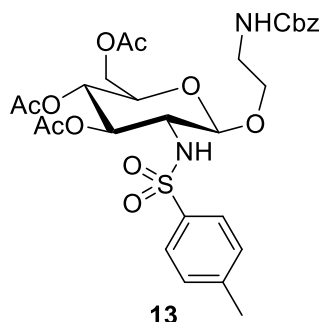
¹H NMR (300.0 MHz, CDCl₃): δ = 7.40 – 7.29 ppm, m, 5 H (aromatic H); δ = 5.35 – 5.16 ppm, m, 3 H (NH (NHCbz, NHTroc), H3); δ = 5.13 – 4.99 ppm, m, 3 H (CH₂ (NHCbz), H3); δ = 4.76 ppm, d, 1 H, J = 11.7 Hz (CHa (NHTroc)); δ = 4.58 ppm, d, 1 H, J = 8.3 Hz (H1); δ = 4.51 ppm, d, 1 H, J = 12.0 Hz (CHb (NHTroc)); δ = 4.24 ppm, dd, 1 H, J = 4.9, 12.3 Hz (H6a); δ = 4.13 ppm, dd, 1 H, J = 2.1, 12.1 Hz (H6b); δ = 3.86 ppm, dd, 1 H, J = 3.9, 10.1 Hz (OCHaCH₂NHCbz); δ = 3.70 - 3.64 ppm, m, 3 H (OCHbCH₂NHCbz, H2, H5); δ = 3.53 - 3.41 ppm, m, 1 H (OCH₂CHaNHCBz); δ = 3.34 ppm, m, 1 H (OCH₂CHbNHCBz); δ = 2.06 ppm, s, 3 H (OCOCH₃); δ = 2.03 ppm, s, 3 H (OCOCH₃); δ = 2.02 ppm, s, 3 H (OCOCH₃).

¹³C NMR (125.7 MHz, CDCl₃): δ = 170.77 ppm, 1 C (OCOCH₃); δ = 170.72 ppm, 1 C (OCOCH₃); δ = 169.46 ppm, 1 C (OCOCH₃); δ = 156.55 ppm, 1 C (NCOO (NHTroc)); δ = 154.29 ppm, 1 C (NCOO (NHCbz)); δ = 136.47 ppm, 1 C (aromatic C); δ = 128.59 ppm, 1 C (aromatic C); δ = 128.24 ppm, 1 C (aromatic C); δ = 128.22 ppm, 1 C (aromatic C); δ = 101.06 ppm, 1 C (C1); δ = 95.43 ppm, 1 C (CCl₃); δ = 74.42 ppm, 1 C (CH₂ (NHTroc)); δ = 71.92 ppm, 2 C (C3, C5); δ = 69.33 ppm, 1 C (OCH₂CH₂NHCbz); δ = 68.45 ppm, 1 C (C4); δ = 66.84 ppm, 1 C (CH₂ (NHCbz)); δ = 61.96 ppm, 1 C (C6); δ = 56.23 ppm, 1 C (C2); δ = 40.73 ppm, 1 C (OCH₂CH₂NHCbz); 1 C (C2); δ = 20.74 ppm, 1 C (OCOCH₃); δ = 20.64 ppm, 2 C (OCOCH₃).

R_f = 0.35 with cyclohexane:EtOAc (1:1).

ESI-MS for C₂₅H₃₁Cl₃N₂O₁₂: m·z⁻¹(M+Na⁺)_{calc} = 679.1; m·z⁻¹(M+Na⁺)_{obs} = 671.0.

(N-(Benzyloxycarbonyl)-2-aminoethyl)-2-deoxy-2-N-tosyl-3,4,6-tri-O-acetyl- β -D-glucopyrannoside



11 (1.1 g, 2.0 mmol) was dissolved in acetic acid (60 ml). Activated zinc (20 g, 260 mmol) was added and the reaction mixture was stirred for 4 h at room temperature. Subsequently, the reaction mixture was filtered over Celite and solvents were removed *in vacuo*. The residue was dissolved in pyridine (4 ml) and tosyl chloride (110 mg, 0.60 mmol) was added slowly under argon atmosphere. The reaction mixture was stirred overnight at room temperature. Solvents were removed *in vacuo* and the residue was purified via flash chromatography (cyclohexane:EtOAc (1:1)) to yield **13** (640 mg, 1.0 mmol, 50%) as a white solid.

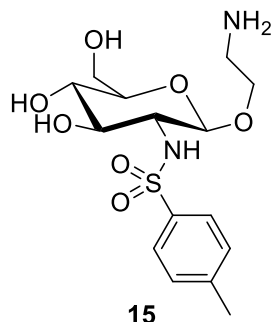
^1H NMR (500.0 MHz, CDCl_3): δ = 7.64 ppm, d, 2 H, J = 8.2 Hz (aromatic H (NHTs)); δ = 7.32 – 7.22 ppm, m, 5 H (aromatic H (NHCbz)); δ = 7.16 ppm, d, 2 H, J = 8.1 Hz (aromatic H (NHTs)); δ = 5.41 ppm, d, 1 H, J = 8.3 Hz (NH (NHTs)); δ = 5.25 ppm, m, 1 H (NH (NHCbz)); δ = 5.03 ppm, s, 2 H (CH_2 (NHCbz)); δ = 4.95 ppm, m, 2 H (H3, H4); δ = 4.27 ppm, d, 1 H, J = 8.2 Hz (H1); δ = 4.14 ppm, dd, 1 H, J = 4.8, 12.3 Hz (H6a); δ = 4.01 ppm, dd, 1 H, J = 2.2, 12.3 Hz (H6b); δ = 3.68 – 3.60 ppm, m, 1 H ($\text{OCH}_a\text{CH}_2\text{NHCbz}$); δ = 3.57 – 3.50 ppm, m, 1 H (H5); δ = 3.46 – 3.37 ppm, m, 1 H (H2); δ = 3.37 – 3.31 ppm, m, 1 H ($\text{OCH}_b\text{CH}_2\text{NHCbz}$); δ = 3.21 – 3.11 ppm, m, 1 H ($\text{OCH}_2\text{CH}_a\text{NHCbz}$); δ = 3.11 – 3.00 ppm, m, 1 H ($\text{OCH}_2\text{CH}_b\text{NHCbz}$); δ = 2.29 ppm, s, 3 H (CH_3 (NHTs)); δ = 1.98 ppm, s, 3 H (OCOCH_3); δ = 1.94 ppm, s, 3 H (OCOCH_3); δ = 1.81 ppm, s, 3 H (OCOCH_3).

^{13}C NMR (125.7 MHz, CDCl_3): δ = 171.41 ppm, 1 C (OCOCH_3); δ = 170.82 ppm, 1 C (OCOCH_3); δ = 169.45 ppm, 1 C (OCOCH_3); δ = 156.77 ppm, 1 C (NCOO (NHCbz)); δ = 143.51 ppm, 1 C (aromatic C (NHTs)); δ = 138.49 ppm, 1 C (aromatic C (NHTs)); δ = 136.72 ppm, 1 C (aromatic C (NHCbz)); δ = 129.55 ppm, 2 C (aromatic C (NHTs)); δ = 128.62 ppm, 3 C (aromatic C (NHCbz)); δ = 128.21 ppm, 2 C (aromatic C (NHCbz)); δ = 127.27 ppm, 2 C (aromatic C (NHTs)); δ = 101.50 ppm, 1 C (C1); δ = 72.95 ppm, 1 C (C3); δ = 71.85 ppm, 1 C (C5); δ = 69.51 ppm, 1 C ($\text{OCH}_2\text{CH}_2\text{NHCbz}$); δ = 68.40 ppm, 1 C (C4); δ = 66.79 ppm, 1 C (CH_2 (NHCbz)); δ = 61.96 ppm, 1 C (6); δ = 58.08 ppm, 1 C (C2); δ = 40.58 ppm, 1 C ($\text{OCH}_2\text{CH}_2\text{NHCbz}$); δ = 26.11 ppm, 1 C (CH_3 (NHTs)); δ = 20.82 ppm, 1 C (OCOCH_3); δ = 20.72 ppm, 1 C (OCOCH_3); δ = 20.70 ppm, 1 C (OCOCH_3).

$R_f = 0.27$ with 10% MeOH in DCM.

ESI-MS for $C_{29}H_{36}N_2O_{12}S$: $m \cdot z^{-1}(M+H^+)_{calc} = 637.2$; $m \cdot z^{-1}(M+H^+)_{obs} = 637.2$.

Aminoethyl-2-deoxy-2-N-tosyl- β -D-glucopyrannoside



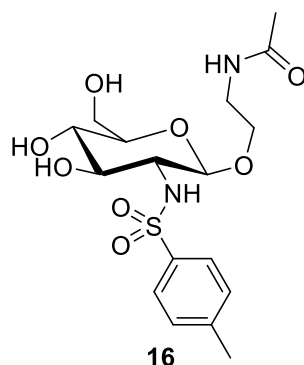
13 (100 mg, 0.16 mmol) was dissolved in MeOH (5 ml) and 0.4 M sodium methanolate in MeOH (43 mg, 0.80 mmol) was added. The reaction mixture was stirred for 2 h at room temperature and solvents were removed *in vacuo*. The residue was dissolved in degassed ethanol and a catalytic amount of Pd/C (10%) was added. The reaction mixture was saturated with hydrogen at atmospheric pressure and stirred overnight at room temperature under hydrogen atmosphere. The reaction mixture was filtered over Celite, washed with EtOAc and solvents were removed *in vacuo*. The residue was purified by reversed-phase HPLC (gradient: 3% to 30% acetonitrile in 0.1% TFA in H₂O in 30 min) to yield **15** (10 mg, 26 μ mol, 16%) as a white solid after lyophilization.

¹H NMR (500.0 MHz, D₂O): $\delta = 7.75$ ppm, d, 2 H, $J = 8.4$ Hz (aromatic H (NHTs)); $\delta = 7.39$ ppm, d, 2 H, $J = 8.5$ Hz (aromatic H (NHTs)); $\delta = 4.41$ ppm, d, 1 H, $J = 8.4$ Hz (H1); $\delta = 3.86$ ppm, dd, 1 H, $J = 2.0, 12.3$ Hz (H6a); $\delta = 3.81$ ppm, ddd, 1 H, $J = 3.2, 8.2, 11.5$ Hz (OCHaCH₂NH₂); $\delta = 3.68$ ppm, dd, 1 H, $J = 5.4, 12.3$ Hz (H6b); $\delta = 3.47$ ppm, ddd, 1 H, $J = 3.5, 5.6, 11.6$ Hz (OCHbCH₂NH₂); $\delta = 3.42 - 3.31$ ppm, m, 3 H (H3, H4, H5); $\delta = 3.16$ ppm, dd, 1 H, $J = 8.4, 10.0$ Hz (H2); $\delta = 3.02$ ppm, ddd, 1 H, $J = 3.2, 5.6, 13.6$ Hz (OCH₂CHaNH₂); $\delta = 2.71$ ppm, ddd, 1 H, $J = 3.5, 8.1, 13.5$ Hz (OCH₂CHbNH₂); $\delta = 2.40$ ppm, s, 3 H (CH₃ (NHTs)).

¹³C NMR (125.7 MHz, D₂O): $\delta = 144.48$ ppm, 1 C (aromatic C (NHTs)); $\delta = 137.61$ ppm, 1 C (aromatic C (NHTs)); $\delta = 129.59$ ppm, 2 C (aromatic C (NHTs)); $\delta = 126.49$ ppm, 2 C (aromatic C (NHTs)); $\delta = 101.17$ ppm, 1 C (C1); $\delta = 75.58$ ppm, 1 C (C4); $\delta = 73.91$ ppm, 1 C (C3); $\delta = 69.71$ ppm, 1 C (C5); $\delta = 65.65$ ppm, 1 C (OCH₂CH₂NH₂); $\delta = 60.48$ ppm, 1 C (C6); $\delta = 59.41$ ppm, 1 C (C2); $\delta = 39.06$ ppm, 1 C (OCH₂CH₂NH₂); $\delta = 20.54$ ppm, 1 C (CH₃ (NHTs)).

HR ESI-MS for $C_{15}H_{24}N_2O_7S$: $m \cdot z^{-1}(M+H^+)_{calc} = 377.138$; $m \cdot z^{-1}(M+H^+)_{obs} = 377.152$.

2-Acetamidoethyl-2-deoxy-2-N-tosyl-β-D-glucopyranoside



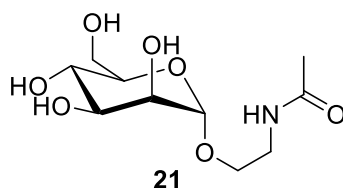
15 (9.8 mg, 26 μmol) was dissolved in MeOH (0.7 ml) and acetic anhydride (50 μl , 490 μmol) was added slowly. The reaction mixture was stirred for 72 h at room temperature, quenched with diethyl amine and solvents were removed *in vacuo*. The residue was purified by reversed-phase HPLC (gradient: 3% to 40% acetonitrile in 0.1% TFA in H₂O in 30 min) to yield **16** (6 mg, 14 μmol , 54%) as a white solid after lyophilization.

¹H NMR (400.1 MHz, D₂O): δ = 7.69 ppm, d, 2 H, J = 8.2 Hz (aromatic H, in proximity of NHSO₂ (NHTs)); δ = 7.35 ppm, d, 2 H, J = 8.4 Hz (aromatic H, in proximity of CH₃ (NHTs)); δ = 4.33 ppm, d, 1 H, J = 8.2 Hz (H1); δ = 3.82 ppm, dd, 1 H, J = 1.5, 12.4 Hz (H6a); δ = 3.64 ppm, m, 1 H (H6b); δ = 3.60 ppm, m, 1 H (OCH_aCH₂NHCOCH₃); δ = 3.38 ppm, m, 1 H (H3); δ = 3.35 – 3.29 ppm, m, 2 H (H4, H5); δ = 3.23 ppm, m, 1 H (OCH_bCH₂NHCOCH₃); δ = 3.08 ppm, dd, 1 H, J = 8.4, 10.1 Hz (H2); δ = 2.99 ppm, ddd, 1 H, J = 4.1, 5.8, 14.5 Hz (OCH₂CH_aNHCOCH₃); δ = 2.80 ppm, ddd, 1 H, J = 3.9, 7.1, 14.3 Hz (OCH₂CH_bNHCOCH₃); δ = 2.35 ppm, s, 3 H (CH₃ (NHTs)); δ = 1.91 ppm, s, 3 H (OCH₂CH₂NHCOCH₃).

¹³C NMR (100.6 MHz, D₂O): δ = 173.84 ppm, 1 C (OCH₂CH₂NHCOCH₃); δ = 144.28 ppm, 1 C (aromatic C (NHTs)); δ = 137.64 ppm, 1 C (aromatic C (NHTs)); δ = 129.50 ppm, 2 C (aromatic C (NHTs)); δ = 126.37 ppm, 1 C (aromatic C (NHTs)); δ = 101.06 ppm, 1 C (C1); δ = 75.56 ppm, 1 C (C5); δ = 74.17 ppm, 1 C (C3); δ = 69.71 ppm, 1 C (C4); δ = 67.87 ppm, 1 C (OCH₂CH₂NHCOCH₃); δ = 60.51 ppm, 1 C (C6); δ = 59.55 ppm, 1 C (C2); δ = 39.04 ppm, 1 C (OCH₂CH₂NHCOCH₃); δ = 21.64 ppm, 1 C (OCH₂CH₂NHCOCH₃); δ = 20.53 ppm, 1 C (CH₃ (NHTs)).

HR ESI-MS for C₁₅H₂₄N₂O₇S: $m \cdot z^{-1}(M+Na^+)_{\text{calc}} = 441.131$; $m \cdot z^{-1}(M+Na^+)_{\text{obs}} = 441.131$.

2-Acetamidoethyl- α -D-mannopyranoside



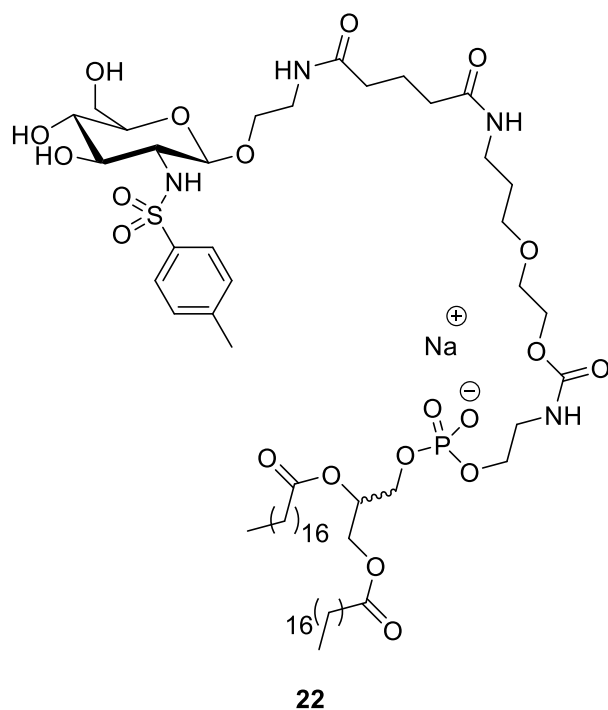
Intermediate **20** was prepared as previously published¹⁰. **20** (23 mg, 103 μ mol) was dissolved in MeOH (700 μ l) and acetic anhydride (10 μ l, 110 μ mol) was added slowly. The reaction mixture was stirred for 24 h at room temperature, quenched with 25 % (w/v) sodium methoxide in methanol and solvents were removed *in vacuo*. The residue was purified by reversed-phase HPLC (gradient: 0% to 10% acetonitrile in 0.1% TFA in H₂O in 40 min) to yield **21** (17 mg, 26 μ mol, 25%) as a white solid after lyophilization.

¹H NMR (400.1 MHz, D₂O): δ = 4.80 ppm, d, 1 H, J = 1.8 Hz (H1); δ = 3.88 ppm, dd, 1 H, J = 1.8, 3.3 Hz (H2); δ = 3.82 ppm, dd, 1 H, J = 2.2, 12.3 Hz (H6a); δ = 3.74 ppm, m, 1 H (H3); δ = 3.71 ppm, m, 1 H (OCH_aCH₂NHCOCH₃); δ = 3.67 ppm, m, 1 H (H6b); δ = 3.59 ppm, m, 1 H (H4); δ = 3.55 ppm, m, 1 H (H5); δ = 3.52 ppm, m, 1 H (OCH_bCH₂NHCOCH₃); δ = 3.52 ppm, ddd, 1 H, J = 3.7, 7.2, 14.4 Hz (OCH₂CH_aNHCOCH₃); δ = 3.31 ppm, ddd, 1 H, J = 3.9, 6.3, 14.4 Hz (OCH₂CH_bNHCOCH₃); δ = 1.95 ppm, s, 3 H (OCH₂CH₂NHCOCH₃).

¹³C NMR (100.6 MHz, D₂O): δ = 174.17 ppm, 1 C (OCH₂CH₂NHCOCH₃); δ = 99.51 ppm, 1 C (C1); δ = 72.69 ppm, 1 C (C5); δ = 70.37 ppm, 1 C (C3); δ = 69.88 ppm, 1 C (C2); δ = 66.55 ppm, 1 C (C4); δ = 65.67 ppm, 1 C (OCH₂CH₂NHCOCH₃); δ = 60.77 ppm, 1 C (C6); δ = 38.90 ppm, 1 C (OCH₂CH₂NHCOCH₃); δ = 21.72 ppm, 1 C (OCH₂CH₂NHCOCH₃).

HR ESI-MS for C₁₅H₂₄N₂O₇S: $m \cdot z^{-1}(M-H^+)_{\text{calc}} = 264.108$; $m \cdot z^{-1}(M-H^+)_{\text{obs}} = 264.109$.

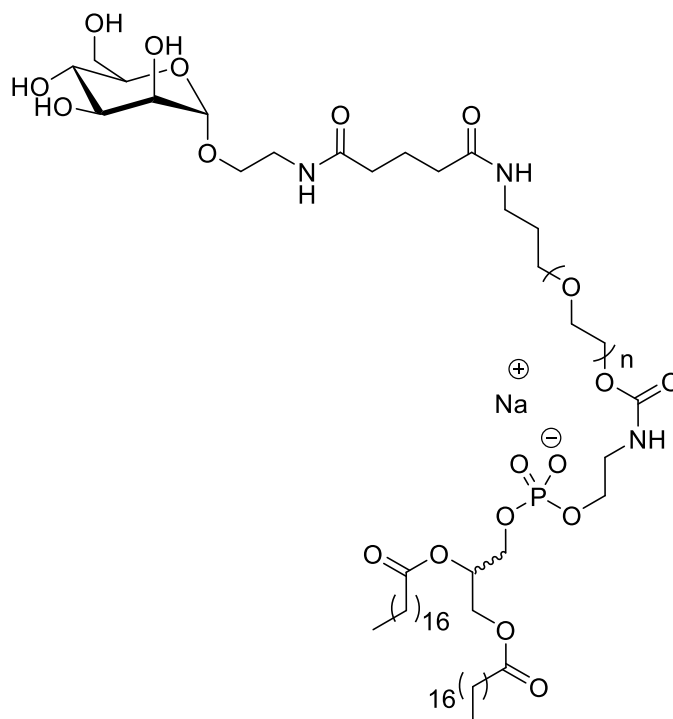
16-PEG-DSPE



NHS-activated PEG-DSPE (3.4 kDa, NOF Europe) (2.8 mg, 900 nmol) was dissolved in DMF (140 μ l) and slowly added to **16** (2.7 mg, 7.20 μ mol) dissolved in 0.1 M NaCO₃H at pH 8.4 (1.2 ml). The reaction mixture was stirred overnight at room temperature. Solvents were removed *in vacuo* and the residue was dissolved in 0.1 M NaCO₃H at pH 8.4 (2.0 ml). Next, the reaction mixture was dialyzed three times against 0.1 M NaCO₃H at pH 8.4 (5.0 ml) and three times against H₂O (5.0 ml). After lyophilization, **22** (2.4 mg, 710 nmol, 79%) was obtained as a white solid. Product formation was analyzed via ¹H NMR and the yield was calculated via the integration of characteristic resonances.

¹H NMR (400.0 MHz, DMSO-*d*₆, characteristic resonances): δ = 7.30 – 7.10 ppm, m, 2 H (aromatic H, **22**); δ = 0.85 ppm, t, 3 H (two times CH₂CH₃).

21-PEG-DSPE



23

NHS-activated PEG-DSPE (3.4kDa, NOF Europe) (2.5 mg, 810 nmol) was dissolved in DMF (130 μ l) and slowly added to **21** (1.5 mg, 6.70 μ mol) dissolved in 0.1 M NaCO₃H at pH 8.4 (1.1 ml). The reaction mixture was stirred overnight at room temperature. Solvents were removed *in vacuo* and the residue was dissolved in 0.1 M NaCO₃H at pH 8.4 (2.0 ml). Next, the reaction mixture was dialyzed three times against 0.1 M NaCO₃H at pH 8.4 (5.0 ml) and three times against H₂O (5.0 ml). After lyophilization, **23** (2.1 mg, 530 nmol, 66%) was obtained as a white solid. Product formation was analyzed via ¹H NMR and the yield was calculated via the integration of characteristic resonances.

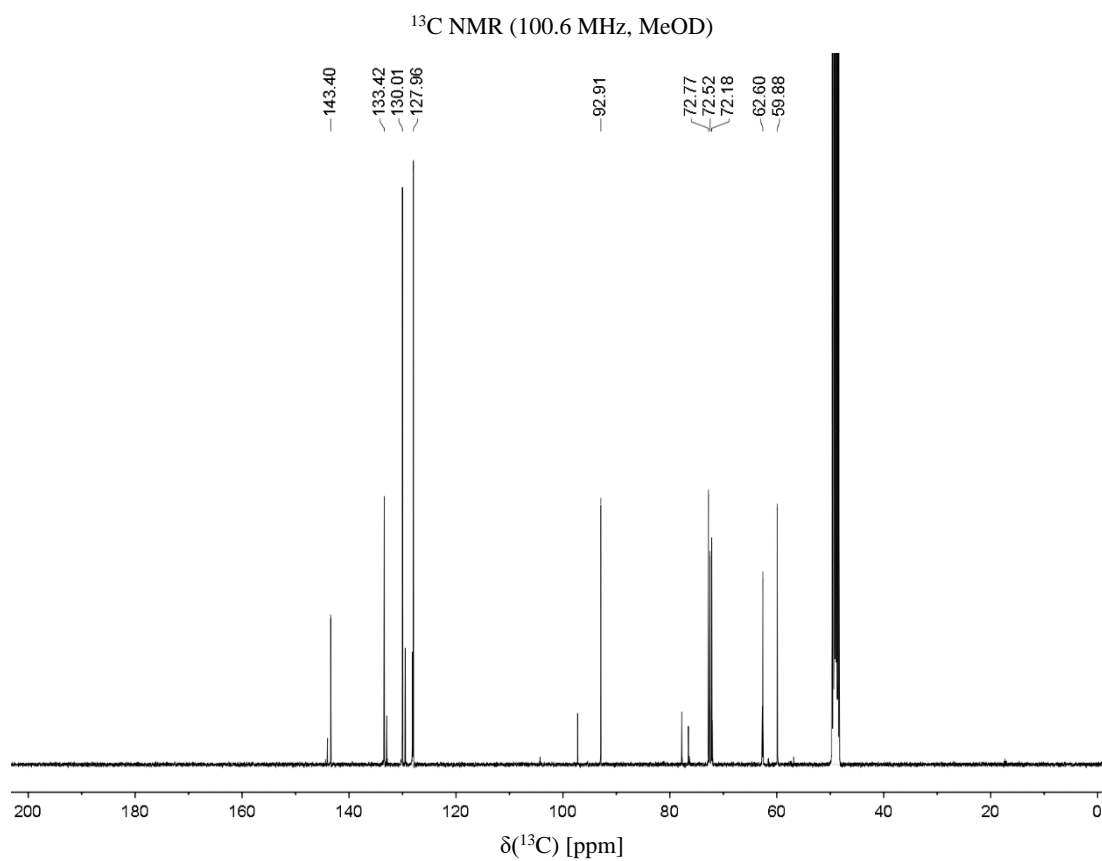
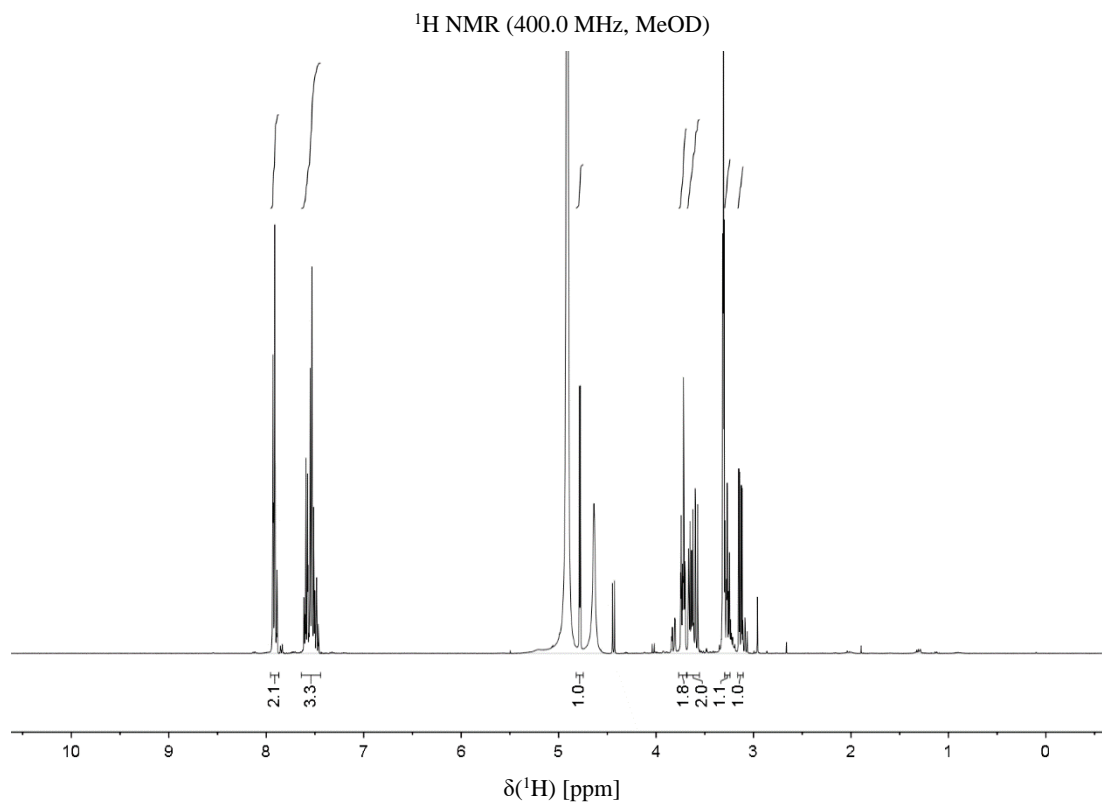
¹H NMR (400.0 MHz, DMSO-*d*₆, characteristic resonances): δ = 4.61 – 4.58 ppm, m, 1 H (H1, **12.29**): δ = 0.85 ppm, t, 3 H (two times CH₂CH₃).

Alexa Fluor 647-PEG-DSPE

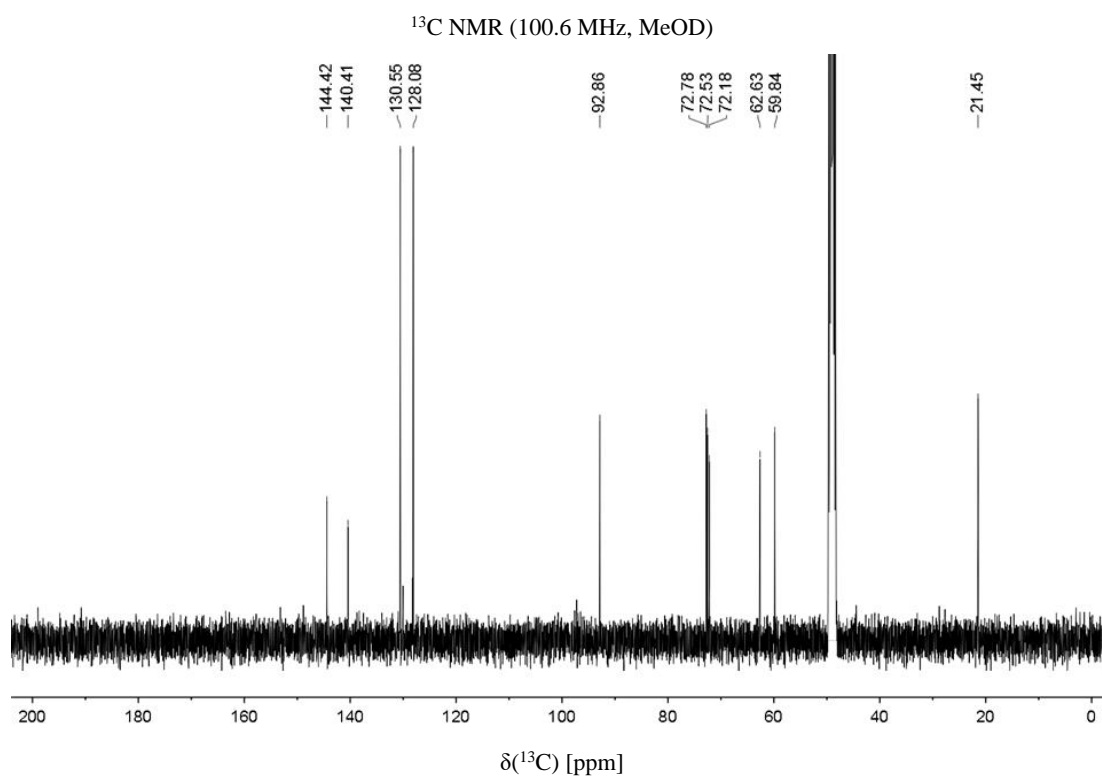
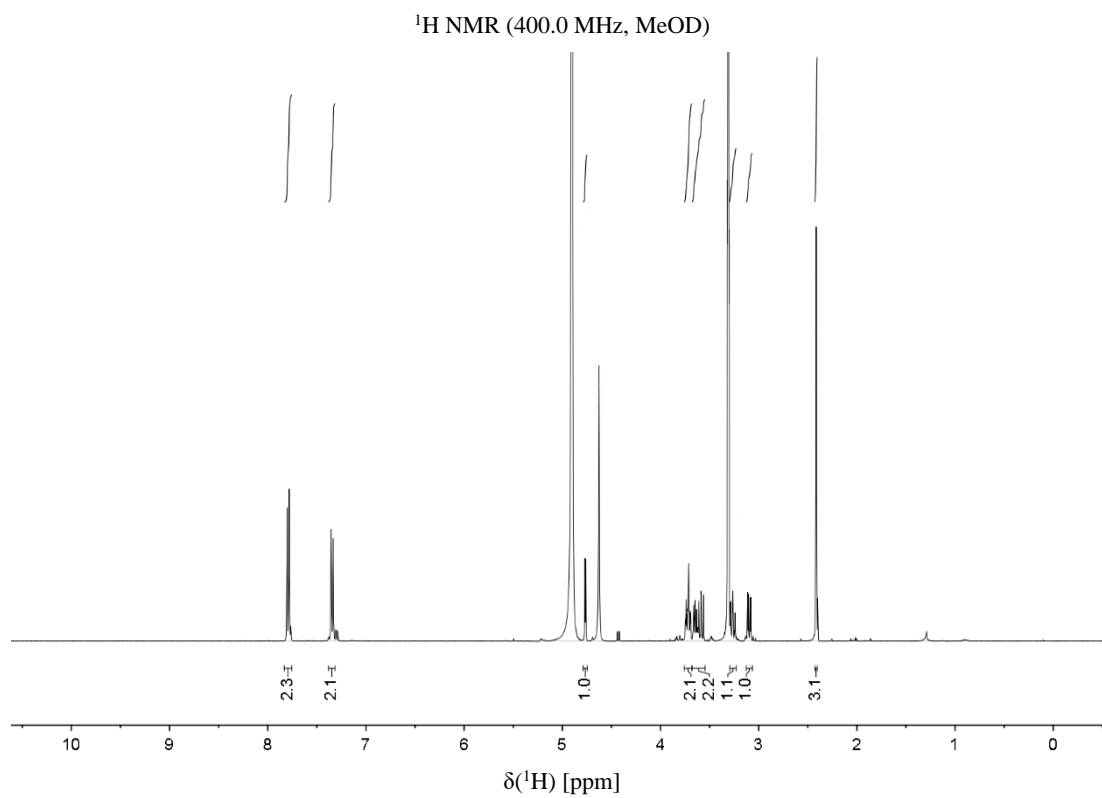
Amino-PEG-DSPE (3.1 kDa, NOF Europe) (1.0 mg, 320 nmol) was dissolved in DMSO (500 μ l) and slowly added to NHS-activated Alexa Fluor 647 (Thermo Scientific) (1.0 mg, 1.6 nmol) dissolved in DMSO (500 μ l). The reaction mixture was stirred overnight at room temperature and protected from light. Solvents were removed by lyophilization and the residue was dissolved in 0.1 M NaCO₃H at pH 8.4 (2.0 ml). Next, the reaction mixture was dialyzed three times against 0.1 M NaCO₃H at pH 8.4 (5.0 ml) and three times against H₂O (5.0 ml). After lyophilization, Alexa Fluor 647-PEG-DSPE (0.9 mg, 240 nmol) was obtained as a red solid.

Synthetic Chemistry – ^1H and ^{13}C NMR Spectra

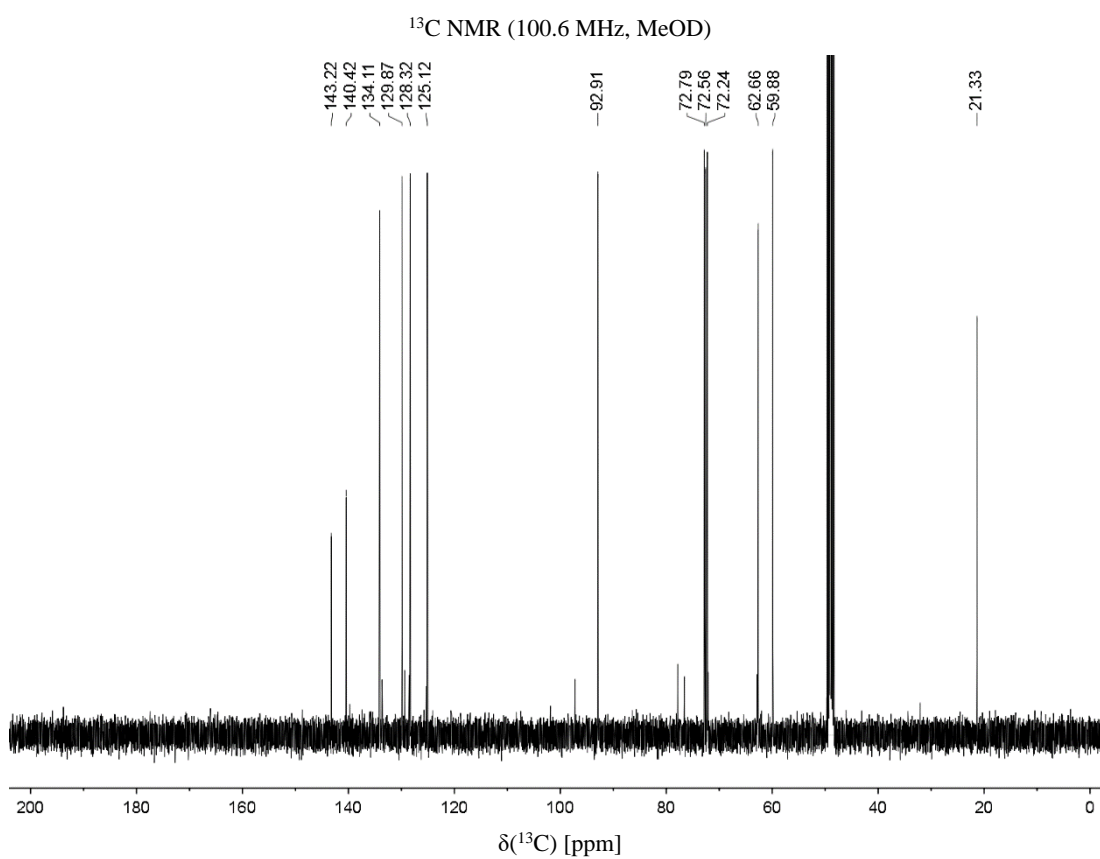
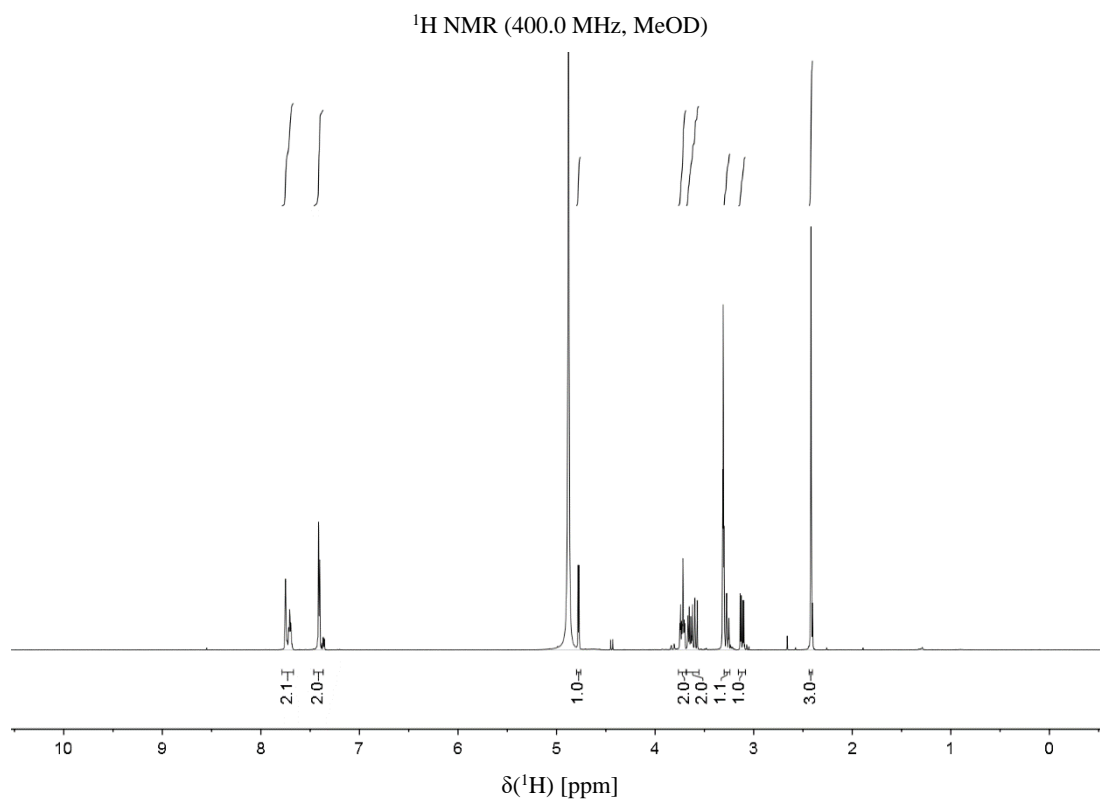
2-deoxy-2-phenylsulfonylamido-D-glucopyranose (1)



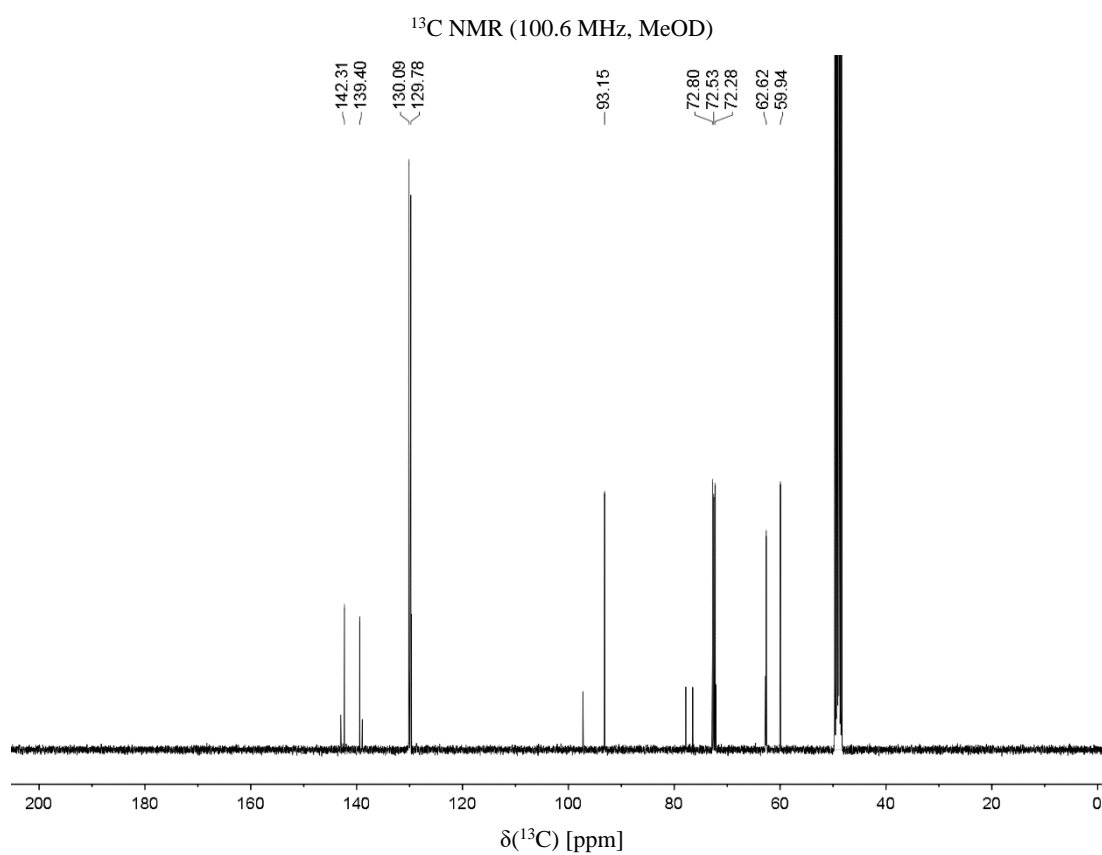
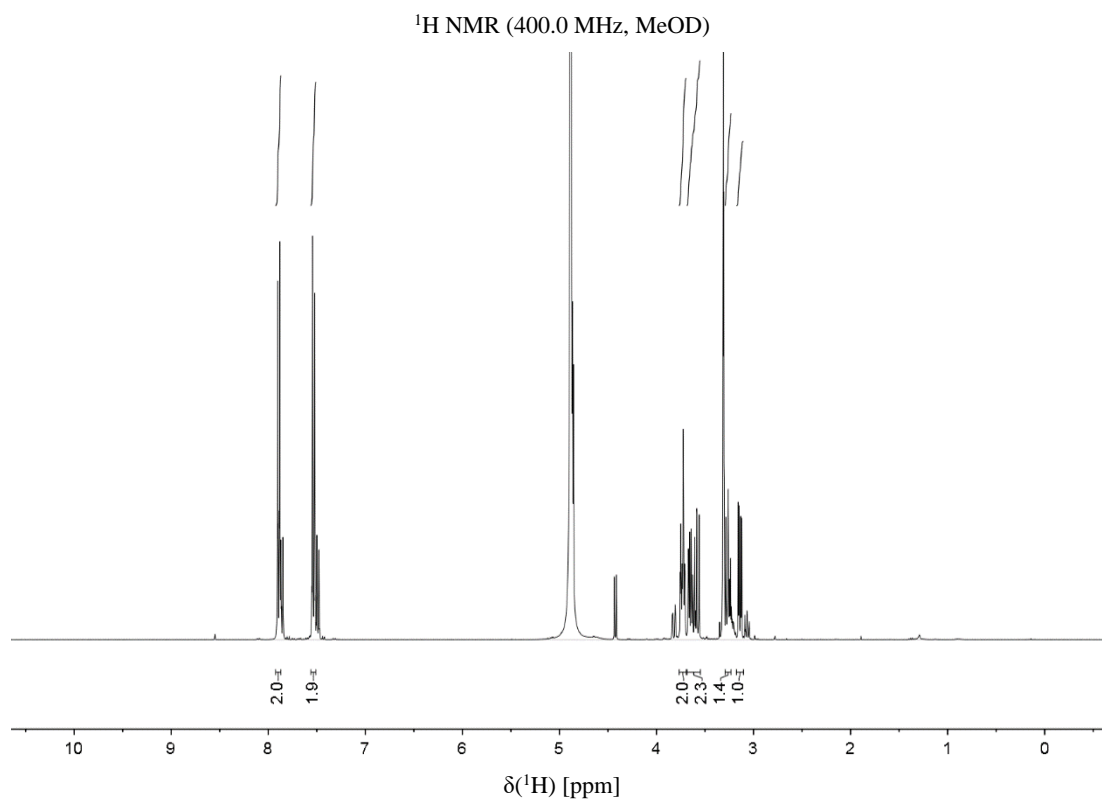
2-deoxy-2-N-tosyl-D-glucopyranose (2)



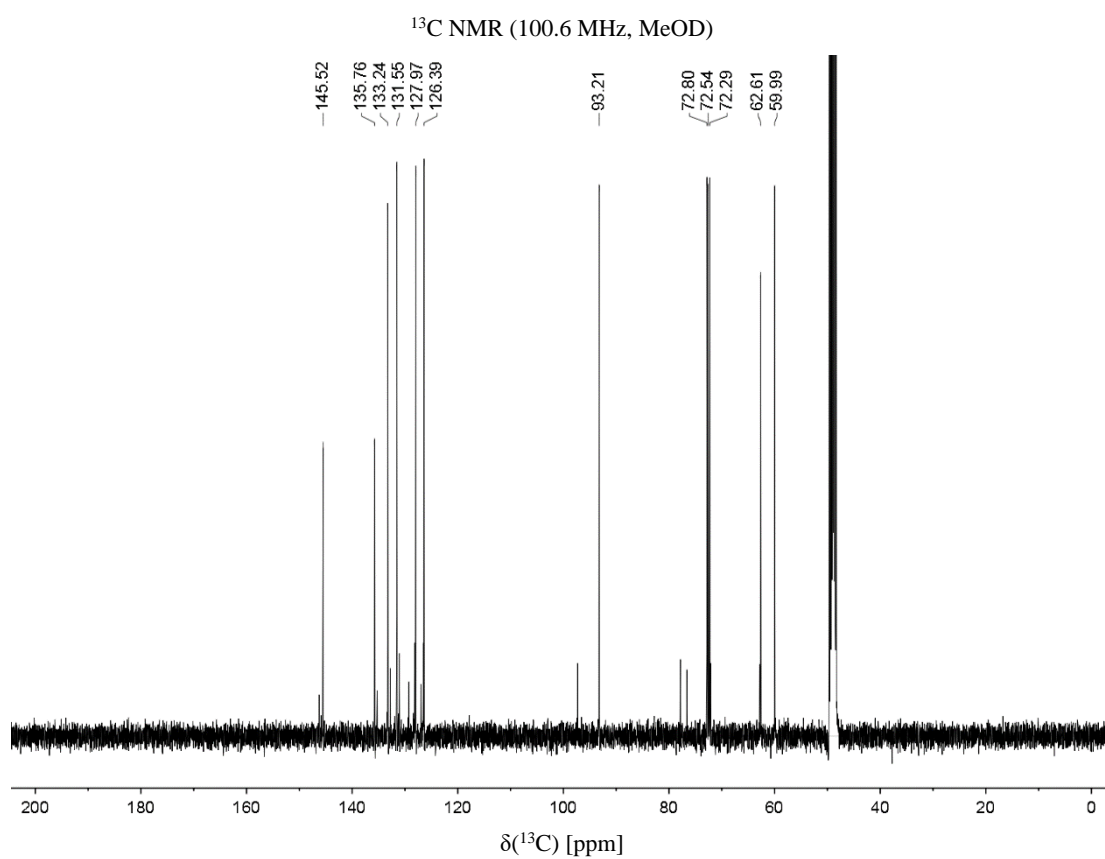
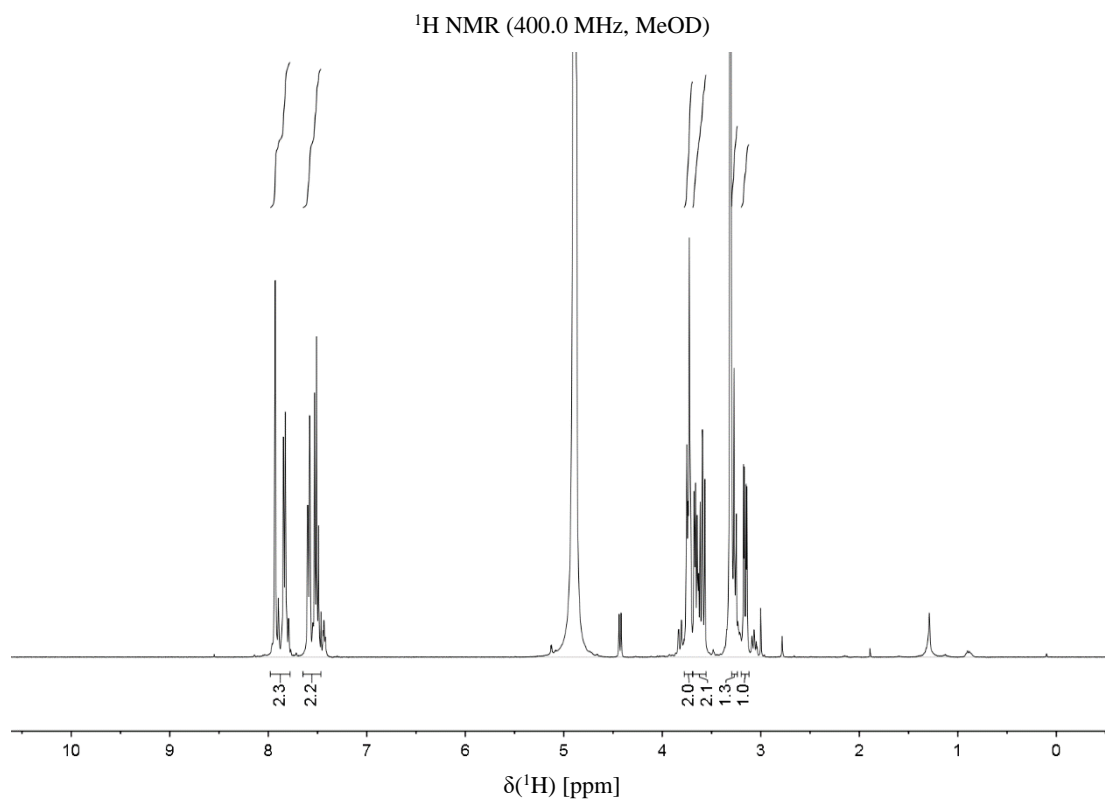
2-deoxy-2-3'-(methyl)phenylsulfonamido-D-glucopyranose (3)



2-deoxy-2-4'-(chloro)phenylsulfonamido-D-glucopyranose (4)

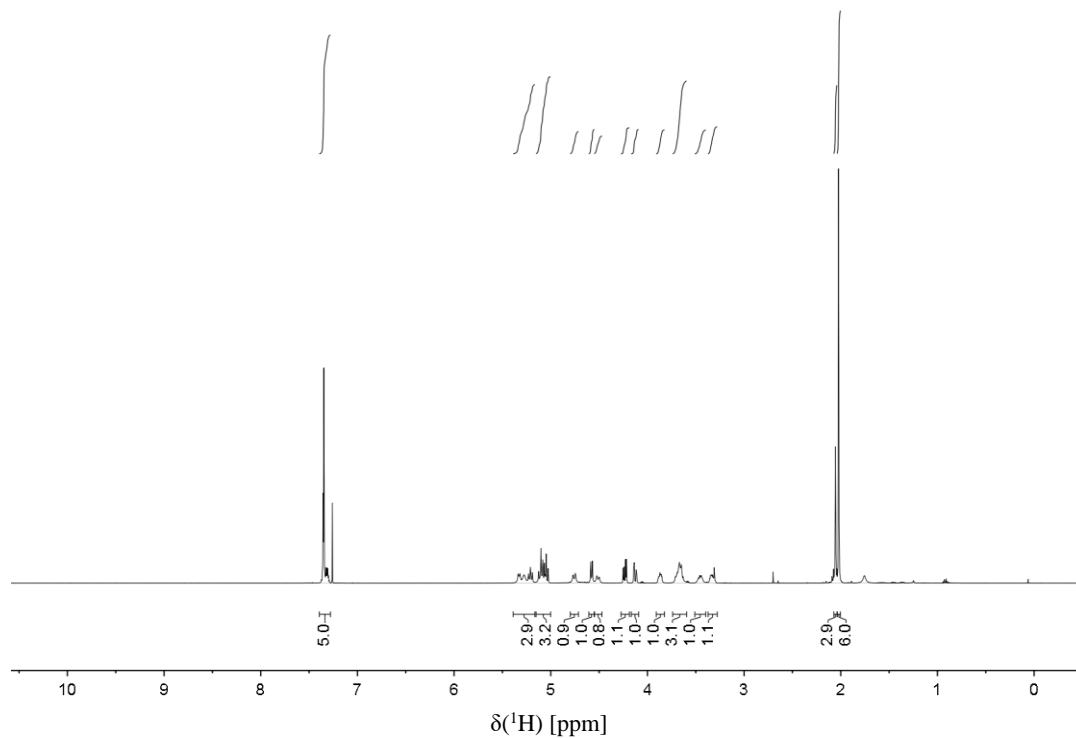


2-deoxy-2-3'-(chloro)phenylsulfonylamido-D-glucopyranose (5)

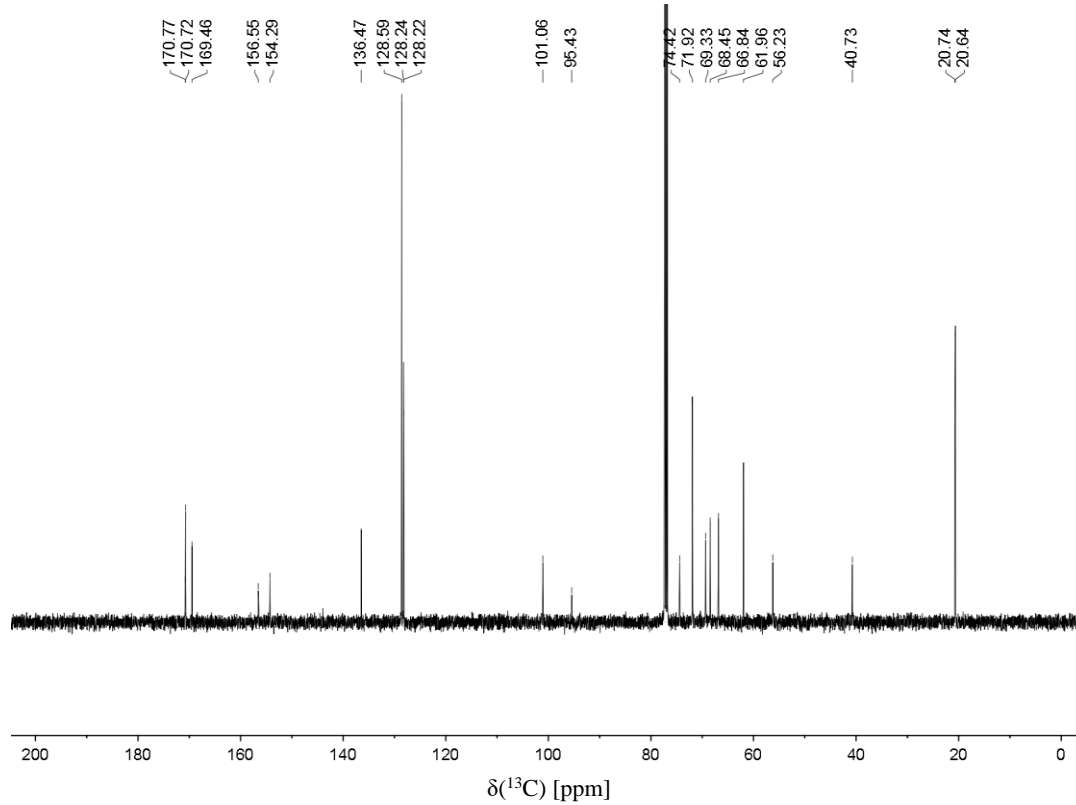


(N-(Benzyloxycarbonyl)-2-aminoethyl)-2-deoxy-2-N-(2,2,2-trichloroethoxy-carbonyl)-3,4,6-tri-O-acetyl-β-D-glucopyranoside (11)

¹H NMR (300.0 MHz, CDCl₃)

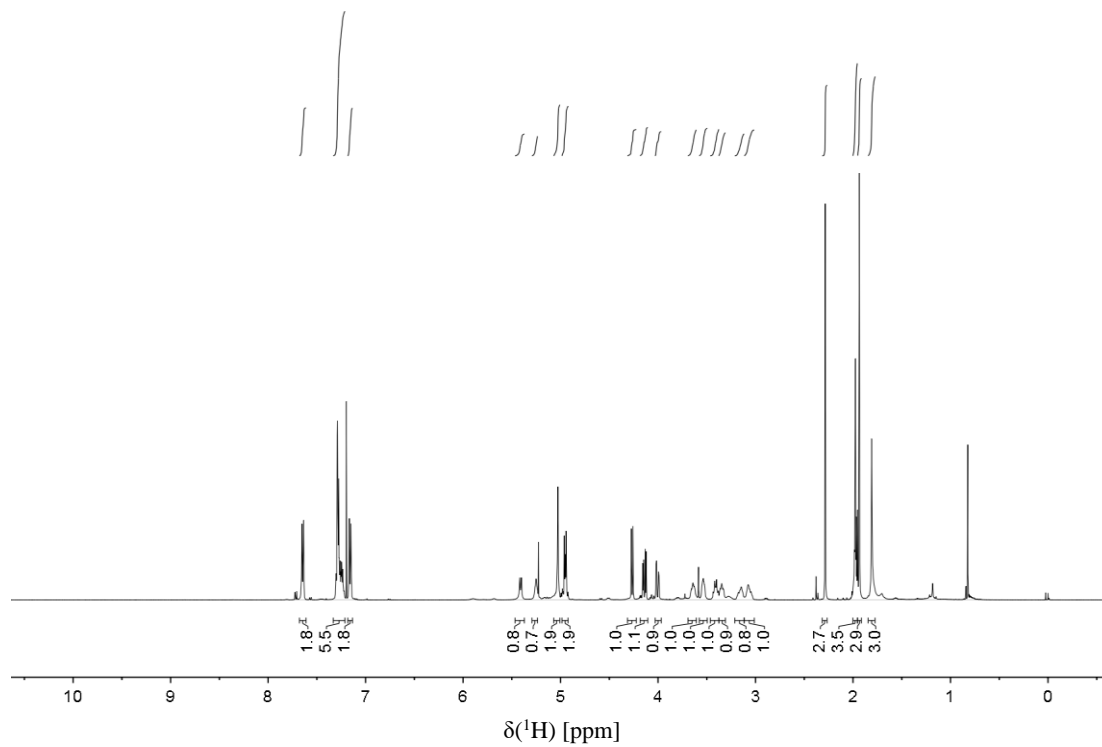


¹³C NMR (125.7 MHz, CDCl₃)

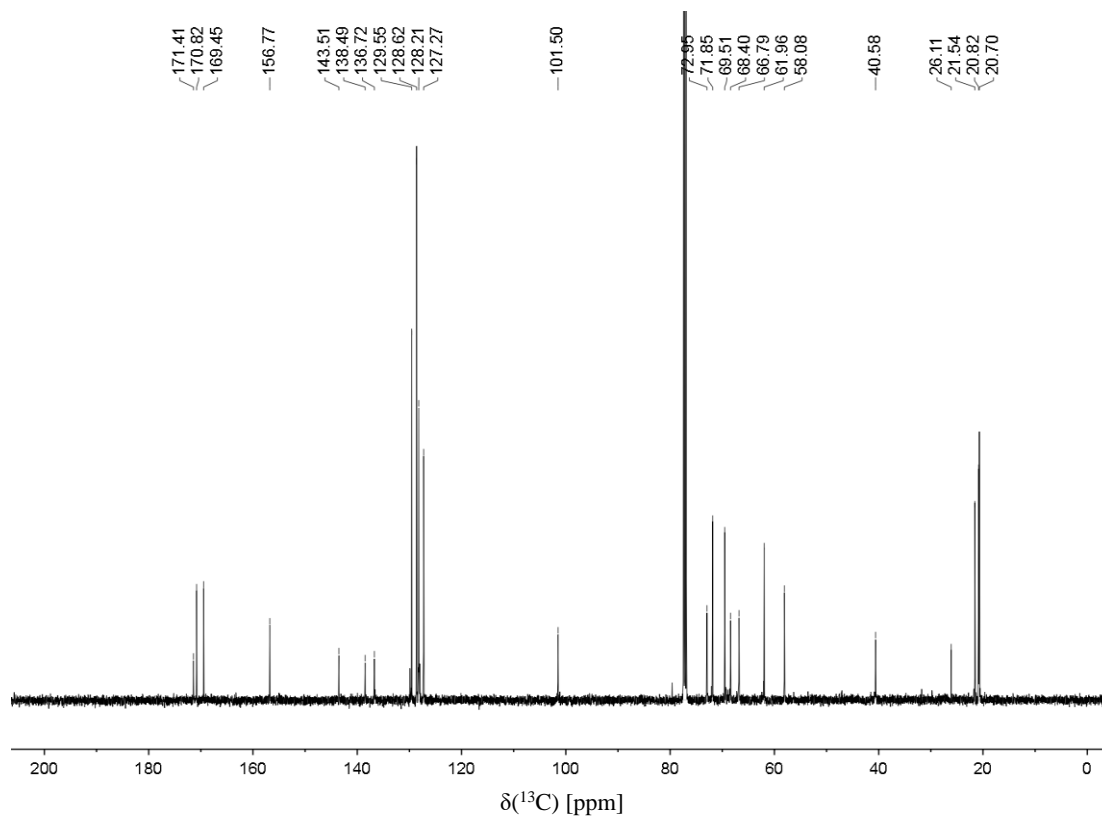


(N-(Benzyloxycarbonyl)-2-aminoethyl)-2-deoxy-2-N-tosyl-3,4,6-tri-O-acetyl- β -D-glucopyranoside (13)

^1H NMR (500.0 MHz, CDCl_3)

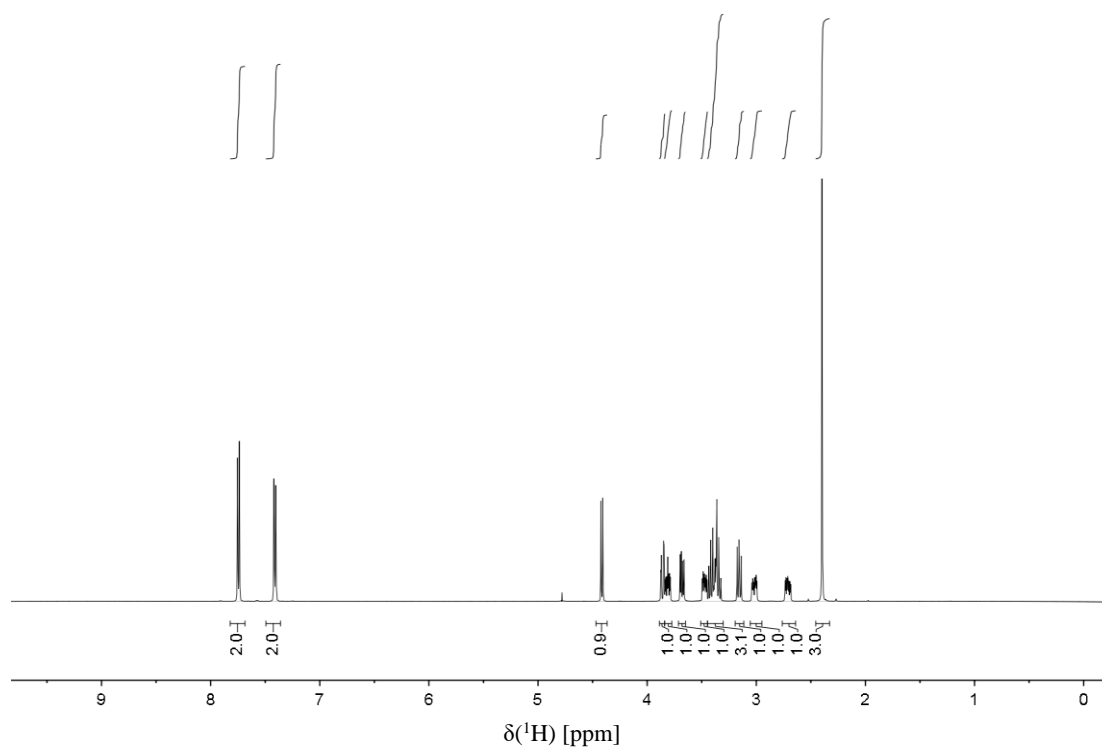


^{13}C NMR (125.7 MHz, CDCl_3)

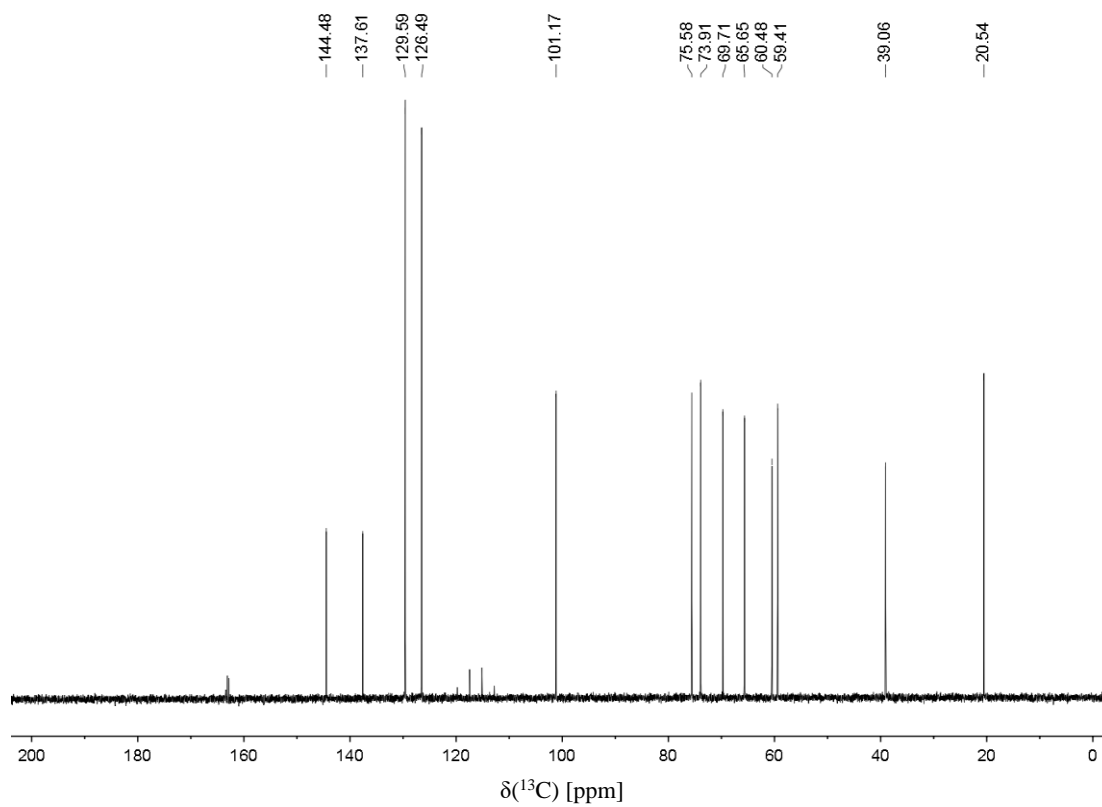


Aminoethyl-2-deoxy-2-N-tosyl-β-D-glucopyranoside (15)

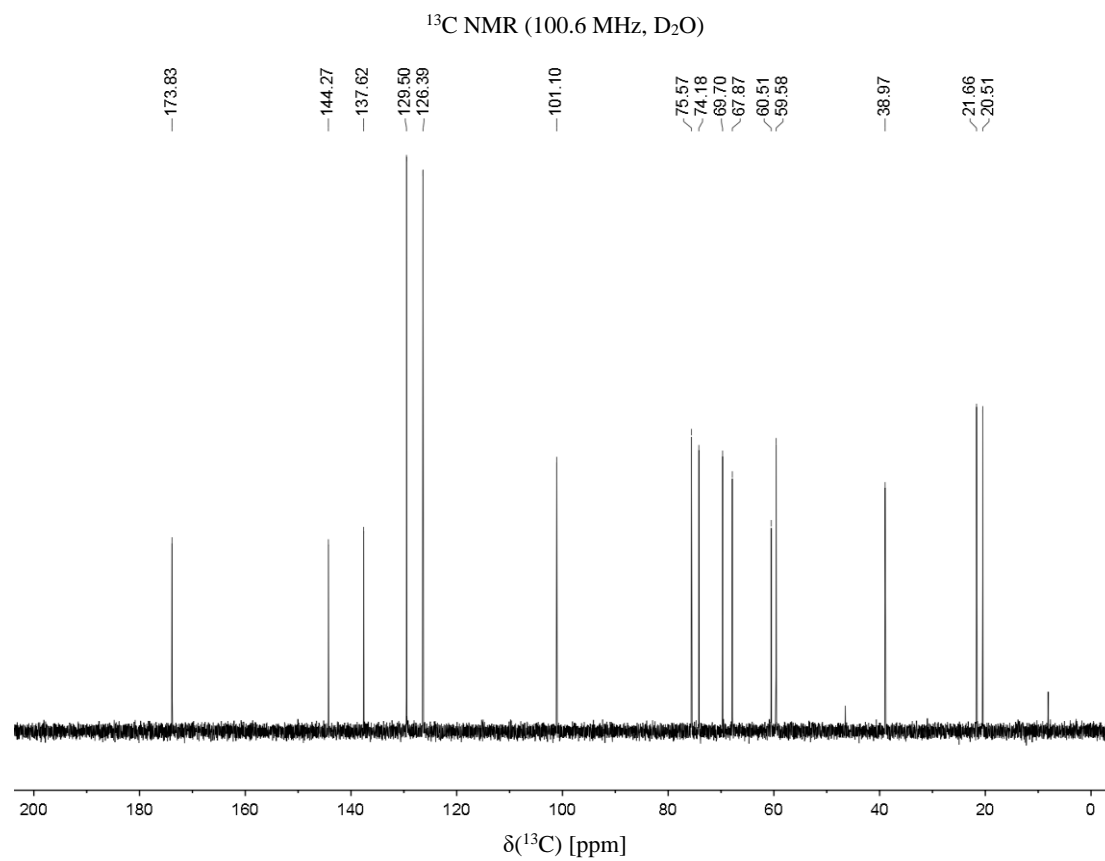
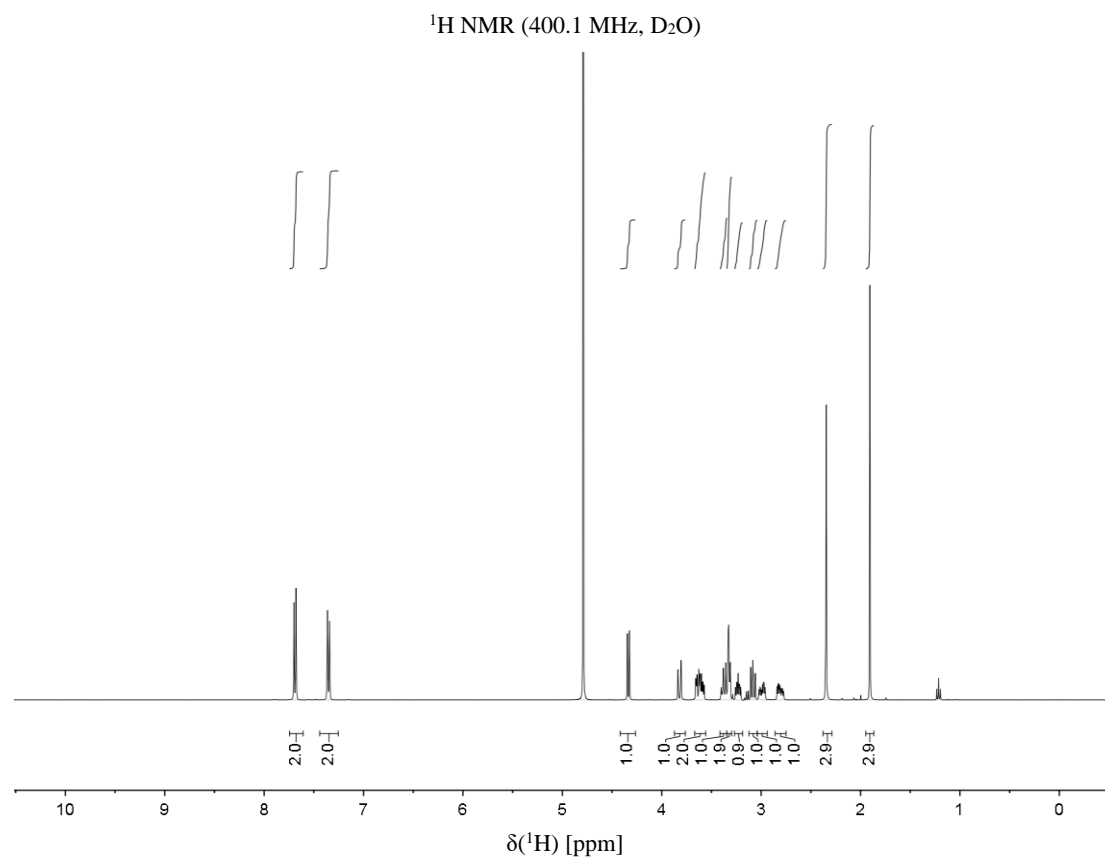
¹H NMR (500.0 MHz, D₂O)



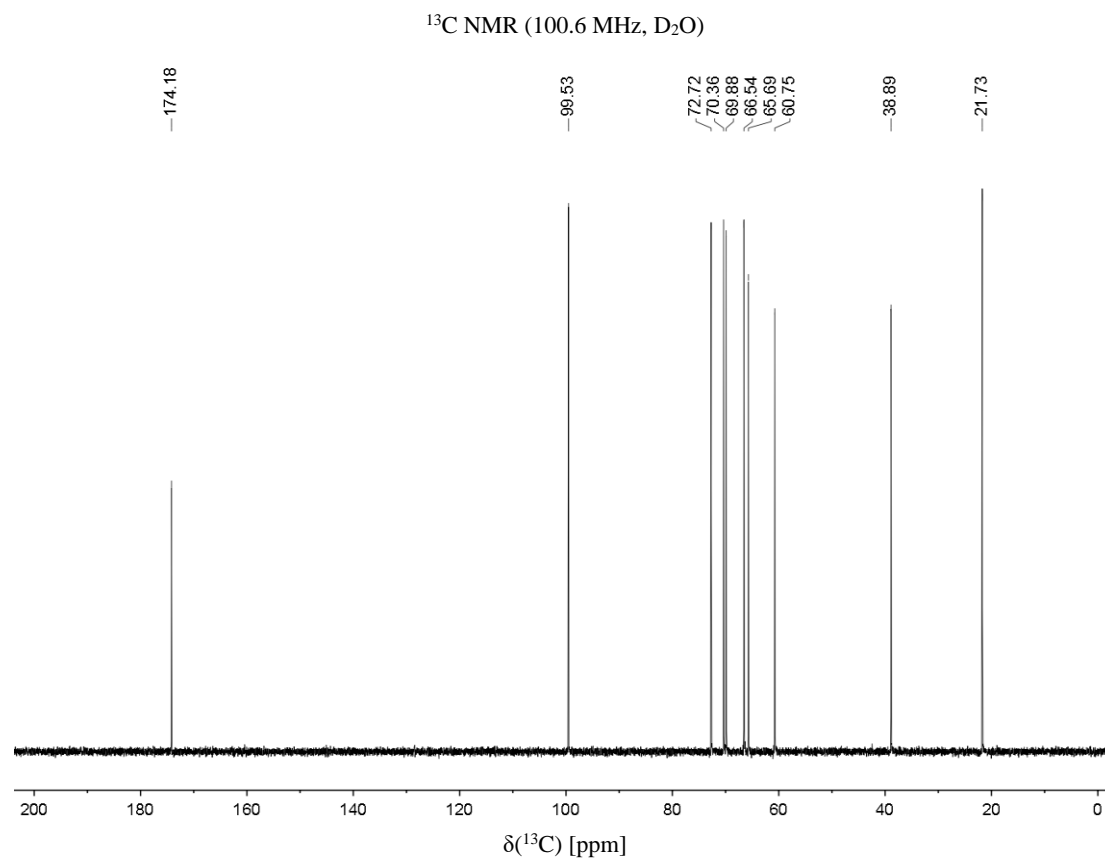
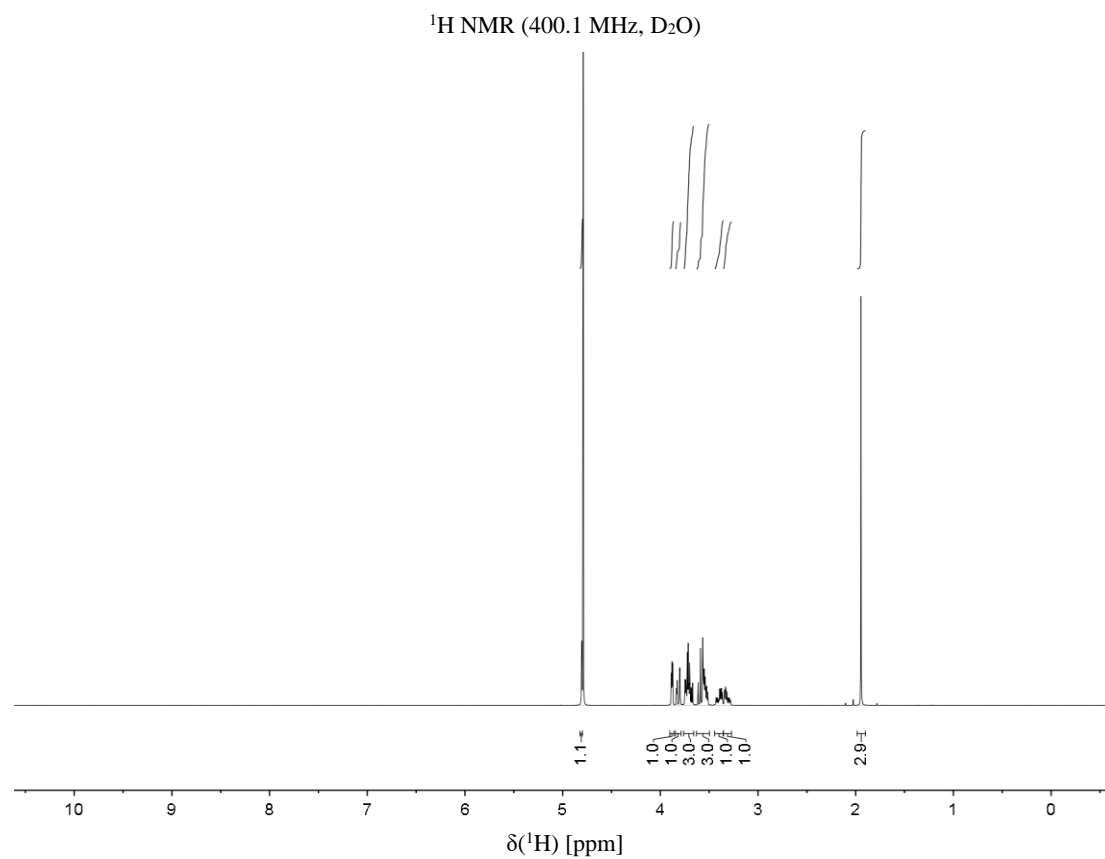
¹³C NMR (125.7 MHz, D₂O)



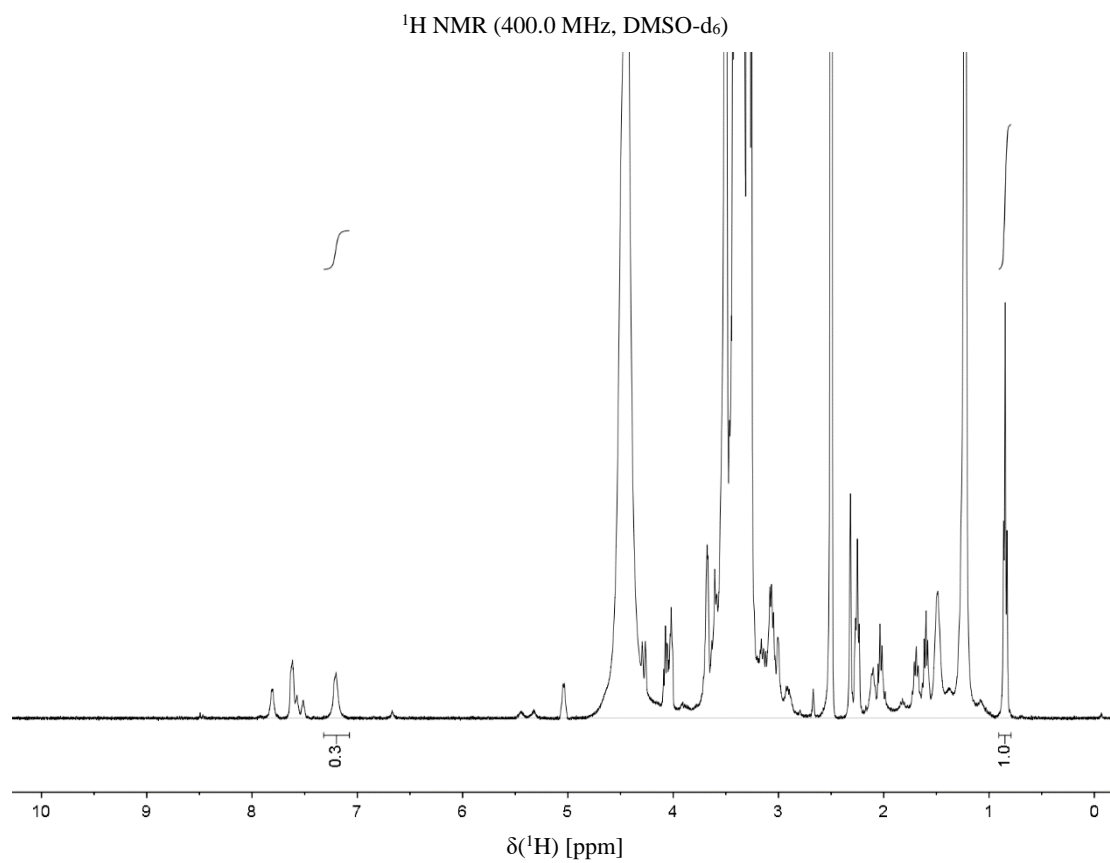
2-Acetamidoethyl-2-deoxy-2-N-tosyl-β-D-glucopyranoside (16)



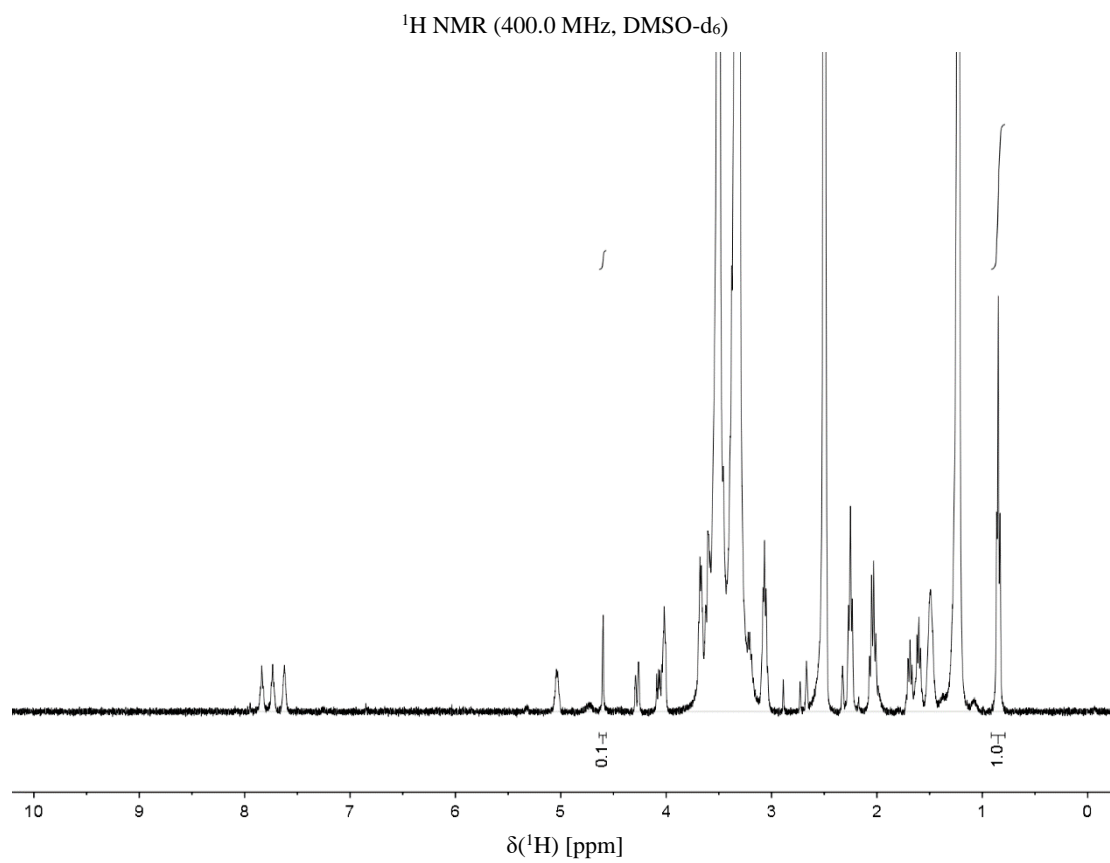
2-Acetamidoethyl- α -D-mannopyranoside (21)



16-PEG-DSPE (22)



21-PEG-DSPE (23)



Receptor Expression and Purification

General remarks. Codon-optimized genes for the expression of Langerin and DC-SIGN in *E. coli* were purchased from GenScript and Life Technologies, respectively. All growth media or chemicals used for receptor expression and purification were purchased from Carl Roth if not stated otherwise.

Langerin extracellular domain. Expression and purification were conducted as previously published¹⁴. Briefly, the trimeric Langerin extracellular domain (ECD) was expressed insolubly in *E. coli* BL21* (DE3) (Invitrogen). Following enzymatic cell lysis, inclusion bodies were harvested and subsequently solubilized. The sample was centrifuged and the Langerin ECD was refolded overnight via rapid dilution. Next, the sample was dialyzed overnight, centrifuged and purified via mannan-agarose affinity chromatography (Sigma Aldrich). For ¹⁹F R₂-filtered NMR and lipid-enzyme-linked lectin assay (Lipid-ELLA) experiments, the buffer was exchanged to 25 mM Tris with 150 mM NaCl and 5 mM CaCl₂ at pH 7.8 using 7 kDa size-exclusion desalting columns (Thermo Scientific). For STD NMR experiments, Langerin ECD samples were dialyzed five times for at least 8 h against H₂O. Subsequently, the H₂O was removed via lyophilization and the residue was stored at -80° C. Prior to STD NMR experiments, the Langerin ECD was dissolved in 25 mM Tris-d₁₁ (EurisoTop) with 100% D₂O, 150 mM NaCl and 5 mM CaCl₂ at pH 7. The concentration of Langerin ECD was determined via UV spectroscopy ($A_{280, 0.1\%} = 2.45$). Purity and monodispersity of Langerin ECD samples were analyzed via SDS PAGE and DLS.

Langerin and DC-SIGN carbohydrate recognition domain. Expression and purification were conducted as previously published¹⁴. Briefly, the monomeric ¹⁵N-labeled Langerin and DC-SIGN carbohydrate recognition domains (CRDs) were expressed insolubly in *E. coli* BL21* (DE3) (Invitrogen). Following enzymatic cell lysis, inclusion bodies were harvested and subsequently solubilized. The sample was centrifuged and the Langerin and DC-SIGN CRDs were refolded overnight via rapid dilution. Next, the sample was dialyzed overnight, centrifuged and purified via StrepTactin affinity chromatography (Iba). After an additional dialysis step overnight, the sample was centrifuged and the buffer was exchanged to 25 mM HEPES with 150 mM NaCl at pH 7.0 using 7 kDa size-exclusion desalting columns (Thermo Scientific) for ¹⁹F R₂-filtered and ¹⁵N HSQC NMR experiments. The concentration of Langerin and DC-SIGN CRDs was determined via UV spectroscopy ($A_{280, 0.1\%} = 3.19$ and $A_{280, 0.1\%} = 2.98$). Purity and monodispersity of Langerin and DC-SIGN CRD samples were analyzed via SDS PAGE and DLS.

¹⁹F R₂-filtered NMR

General remarks. ¹⁹F R₂-filtered NMR experiments were conducted on a PremiumCompact 600 MHz spectrometer (Agilent). Spectra were processed in MestReNova and data analysis was performed with OriginPro^{13, 15}. Experiments with the Langerin ECD were performed at a receptor concentration of 50 μM in 25 mM Tris with 10% D₂O, 150 mM NaCl and 5 mM CaCl₂ at pH 7.8 and 25° C. Experiments

with the DC-SIGN CRD were performed at a receptor concentration of 50 μM in 25 mM HEPES with 10% D_2O , 150 mM NaCl and 5 mM CaCl_2 at pH 7.0 and 25°C. TFA served as an internal reference at a concentration of 50 μM . Apparent relaxation rates $R_{2,\text{obs}}$ for the reporter ligand were determined using the CPMG pulse sequence as previously published³⁻⁵.

Assay development for DC-SIGN. The ^{19}F R_2 -filtered NMR reporter displacement assay for DC-SIGN was developed following the procedure previously published for Langerin³. Briefly, the K_D value and the relaxation rate in bound state $R_{2,\text{b}}$ were determined at five concentrations $[\text{L}]_{\text{T}}$ of reporter ligand **24** in three independent titration experiments. Samples were prepared via serial dilution. The addition of 10 mM EDTA served to validate the Ca^{2+} -dependency of the interaction between DC-SIGN and the reporter ligand. To ensure the validity of the equations for K_D and K_I determination, the chemical exchange contribution $R_{2,\text{ex}}$ was estimated by ^{19}F NMR relaxation dispersion experiments at a reporter ligand concentration of 0.1 mM in presence of receptor.

K_I determination. K_I values were determined as previously published for Langerin³. Briefly, titration experiments were conducted at a concentration of 0.1 mM of reporter ligand **24** at five competitor concentrations $[\text{I}]_{\text{T}}$. Samples were prepared via serial dilution. For the acids GlcNS, GlcNAc-6-OS and GlcNS-6-OS the pH values were monitored and adjusted to 7.8 if necessary.

^{15}N HSQC NMR

General remarks. ^{15}N HSQC NMR experiments were conducted on an Ascend 700 MHz spectrometer (Bruker)¹⁶. Spectra were processed in NMRPipe¹⁷. Data analysis was performed using CCPN Analysis, MatLab and OriginPro^{15, 18-19}. Experiments with the Langerin CRD were performed at a receptor concentration of 100 μM in 25 mM HEPES with 10% D_2O , 150 mM NaCl and 5 mM CaCl_2 at pH 7.8 and 25° C. DSS- d_6 served as an internal reference at a concentration of 100 μM . Spectra were referenced via the internal spectrometer reference. Spectra were acquired with 128 increments and 32 scans per increments for 150 μl samples in 3 mm sample tubes. The relaxation delay d_1 was set to 1.4 s and the acquisition time t_{acq} was set to 100 ms. The W5 Watergate pulse sequence was used for solvent suppression²⁰. The used resonance assignment for the Langerin CRD has been published previously¹.

K_D determination. K_D values were determined in titration experiments at six ligand concentrations $[\text{L}]_{\text{T}}$. Samples were prepared via serial dilution. Chemical shift perturbations CSPs for Langerin CRD resonances in the fast or fast-to-intermediate exchange regime observed upon titration with ligand were calculated via Equation 1²¹.

$$CSP = \sqrt{\frac{\delta(^1H) + (0.15\delta(^{15}N))^2}{2}}$$

Equation 1

A standard deviation σ of 0.02 ppm was previously determined for the measurement of chemical shifts in ^{15}N HSQC NMR experiments with the Langerin CRD¹. Accordingly, only assigned resonances that displayed CSP values higher than a threshold of 2σ at the highest ligand concentration were selected for the determination of K_D values via Equation 2 in a global two parameter fit²¹. Standard errors were derived directly from the fitting procedures. Additionally, resonances that displayed line broadening $\Delta\nu_{0.5}$ larger than 10 Hz upon titration in either the ^1H or the ^{15}N dimension were not considered for the determination of K_D values. CSP_{max} represents the CSP value observed upon saturation of the binding site.

$$\text{CSP} = \text{CSP}_{\text{max}} p_b$$

with

$$p_b = \frac{[P]_T + [L]_T + K_D - \sqrt{([P]_T + [L]_T + K_D)^2 - 4[P]_T[L]_T}}{2[P]_T}$$

Equation 2

For resonances assumed to be in the slow exchange regime upon titration, K_D values were derived from integrals V_b and V_f corresponding to the bound and free state of the Langerin CRD, respectively. V values served to calculate the bound fraction of the receptor p_b via Equation 3. Integrals V were normalized via integral V of the N -terminal K347 and served to calculate the bound fraction of the receptor p_b via Equation 3. For these calculations, only resonances for which the bound state could be assigned were considered. Selected data points displaying a low SNR or issues with the baseline correction were treated as outliers and not considered for the determination of p_b values. Next, a one parameter fit of Equation 3 to mean p_b values served to determine K_D values.

$$\frac{V_b}{V_b + V_f} = p_b$$

with

$$p_b = \frac{[P]_T + [L]_T + K_D - \sqrt{([P]_T + [L]_T + K_D)^2 - 4[P]_T[L]_T}}{2[P]_T}$$

Equation 3

Binding mode analysis. Based on the resonance assignment, CSP values observed at maximal ligand concentrations $[L]_T$ were mapped on the X-ray structure of the Langerin CRD (PDB code: 4N32) using Matlab's Bioinformatics Toolbox via substitution of the B-factor values^{7, 22}. The CSP patterns obtained were visualized in MOE using Chain B of the Langerin CRD in complex with GlcNAc²³. Model quality was maintained using MOE's Structure Preparation followed by the simulation of protonation states and the hydrogen bond network of the complex with MOE's Protonate 3D. Receptor surfaces were visualized in Connolly representation²⁴.

STD NMR

General remarks. STD NMR experiments were conducted on a PremiumCompact 600 MHz spectrometer (Agilent)²⁵. Spectra were processed in MestReNova and data analysis was performed with OriginPro^{13, 15}. Experiments with the Langerin ECD were conducted at a receptor concentration of 50 μM in 25 mM Tris- d_{11} (Eurisotope) with 100% D_2O , 150 mM NaCl and 5 mM CaCl_2 at pH 7.8 and 25° C. Experiments were repeated in absence of receptor to exclude STD effects due to direct saturation of ligands. Residual H_2O or TSP- d_6 at 0.1 mM served as an internal reference. Spectra were recorded in 5 mm sample tubes at sample volumes of 500 μl . Saturation was implemented via a train of 50 ms Gauss pulses at varying saturation times t_{sat} . The on-resonance irradiation frequency ν_{sat} was set to 0.0 ppm and the off-resonance irradiation frequency ν_{ref} was set to 80.0 ppm. The acquisition time t_{acq} was set to 2.0 s and the DPGSE pulse sequence was utilized for solvent suppression²⁶. Receptor resonances were suppressed using a $T_{1,\rho}$ filter at a relaxation time τ of 35 ms.

The methods for the EDTA control with **16** deviate as follows: STD NMR experiments were conducted on an Ascend 700 MHz spectrometer (Bruker)²⁵. Experiments with the Langerin ECD were conducted at a receptor concentration of 20 μM . The 3-9-19 WATERGATE pulse sequence was utilized for solvent suppression and no $T_{1,\rho}$ filter was used²⁷.

EDTA control. The experiment was conducted at 500 μM **16** and in presence of 10 mM EDTA- d_{16} . For each spectrum 2048 scans were recorded. The relaxation delay d_1 was set to 2 s and the saturation time t_{sat} was set to 2.00 s.

Epitope mapping. The binding epitope for **16** was determined at a concentration of 500 μM . For each spectrum 512 scans were recorded. The relaxation delay d_1 was set to 6 s and spectra were recorded at 5 different saturation time t_{sat} varying from 0.25 to 6.00 s. Equation 4 served to derive the STD effect STD for each analyzed resonance from the corresponding on- and off-resonance spectra²⁸. I_0 represents the integral of a resonance in the off-resonance spectrum and I_{sat} represents the integral of a resonance in the on-resonance spectrum.

$$STD = \frac{I_0 - I_{\text{sat}}}{I_0}$$

Equation 4

The apparent saturation rate k_{sat} and the maximal STD effect STD_{max} were derived from Equation 5 in a two parameter fit²⁹. Standard errors were derived directly from the fitting procedures. These parameters were used to calculate the initial slope of the STD build-up curves STD'_0 via Equation 6. STD'_0 values were normalized and mapped on the corresponding ligand structure. Only resonances for which at least part of a multiplet was isolated were considered for the epitope mapping.

$$STD = STD_{max}(1 - e^{-k_{sat}t_{sat}})$$

Equation 5

$$STD'_0 = STD_{max}k_{sat}$$

Equation 6

Molecular Modelling

General remarks. Molecular modelling procedures were performed in MOE²³. Deviations from default options and parameters are noted. The AMBER10:EHT force field was selected for the refinement of docking poses and the hydrogen bond network while the MMFF94x force field was utilized for the generation conformers³⁰⁻³². Receptor surfaces were visualized in Connolly representation²⁴.

Development of the pharmacophore model and preparation of the Langerin complex. A structural alignment of Langerin carbohydrate binding sites in complex with GlcNAc was performed (PDB codes: 4N32)⁷. Based on this visualization, a pharmacophore model was defined with features for O3, O4 and O5 of the Glc scaffold. The spatial constraint on the O3 and O4 was defined by a sphere with a radius r of 0.5 Å while the position of O5 was constrained by a sphere with a radius r of 1.0 Å. Chain B of the Langerin CRD in complex with GlcNAc served as the structural basis for the conducted molecular docking study. Additionally, an alternative conformation for K313 observed for the Langerin complex with Gal-6-OS was modeled and included in the study⁸. Overall model quality and protein geometry were evaluated and maintained using MOE's Structure Preparation. Next, protonation states and the hydrogen bond network of the complex were simulated with MOE's Protonate 3D followed by the removal of all solvent molecules.

Molecular docking. Conformations for **16** were generated utilizing MOE's Conformation Import. A pharmacophore-based placement method was utilized to generate docking poses that we scored using the London ΔG function. Highly scored poses were refined utilizing molecular mechanics simulations, rescored via the GBIV/WSA ΔG function, filtered using the pharmacophore model and written into the output database³³. Conformational flexibility of the carbohydrate binding site was accounted for by introducing B-factor-derived tethers to side chain atoms. Refined docking poses were ranked according to their the GBIV/WSA ΔG score and evaluated visually in the context of the conducted ¹⁵N HSQC and STD NMR experiments.

Liposomal Formulation

PEGylated liposomes were prepared via thin film hydration and subsequent pore extrusion as previously published³⁴. Briefly, non-targeted liposomes were formulated from a mixture of DSPC:cholesterol:PEG-DSPE:Alexa Fluor 647-PEG-DSPE (57:38:4.75:0.25). For targeted liposomes,

the PEG-DSPE was substituted with glycolipids **22** or **23** at varying ratios. PEG-DSPE (3.0 kDa, NOF Europe), **22** or **23** were dissolved in DMSO, added to a round bottom flask and lyophilized. Next, DSPC (NOF Europe) and cholesterol (Sigma Aldrich) were dissolved in chloroform, added to the test tube and the solvent was removed *in vacuo*. The residue was dissolved in PBS and the mixture was vortexed and sonicated repeatedly until a homogeneous suspension was obtained. Unilamellar liposomes were prepared using a pore extruder (Avanti Polar Lipids) with polycarbonate membranes of 800, 400, 200 and finally 100 nm pore size (Avanti Polar Lipids). Liposomes were characterized by DLS and electrophoresis experiments to determine their Z potential. Liposomes were stored at 4° C. Non-targeted liposomes and liposomes **23** were characterized in ¹H NMR experiments at a total lipid concentration [Lipid]_T of 1.5 mM in PBS at 25° C.

Doxorubicin was encapsulated into liposomes as previously described³⁴. Briefly, the thin film was prepared as described above and dissolved in 250 mM ammonium sulfate. Unilamellar liposomes were prepared using a pore extruder (Avanti Polar Lipids) with polycarbonate membranes of 200 and 100 nm pore size (Avanti Polar Lipids). After dialysis against 290 mM glucose overnight at 4°C, doxorubicin was added at 1:4 (doxorubicin:phospholipid, w:w) and incubated for 40 min at 65°C. Liposomes were purified from free doxorubicin via size exclusion chromatography (CL-4B Sepharose, Sigma Aldrich) in 5% sucrose. The amount of encapsulated doxorubicin was determined via fluorescence spectroscopy ($\lambda_{\text{ex}} = 485 \text{ nm}$ and $\lambda_{\text{em}} = 590 \text{ nm}$) after lysis of the liposomes in 0.5% Triton X-100.

Lipid-ELLA

The Lipid-ELLA was conducted as previously published³⁵. Briefly, 1 mg·l⁻¹ of PEG-DSPE (3.0 kDa, NOF Europe), **22** or **23** or unconjugated PEG-DSPE in 100 mM Tris (50 μl per well) at pH 8.9 and 4° C were added to a 384 well MaxiSorp plate (Nunc) and incubated overnight to immobilize the PEGylated lipids. After removal of the supernatant, the wells were blocked with 2% BSA in 25 mM Tris with 150 mM NaCl and 0.1% Tween-20 (70 μl per well) at pH 7.6 and room 25° C for 1 h. Next, the wells were washed three times using 25 mM HEPES with 150 mM NaCl, 5 mM CaCl₂ and 0.01% Tween-20 at pH 7.6 and room temperature (100 μl per well). The wells were incubated with Langerin ECD in 25 mM HEPES with 150 mM NaCl, 5 mM CaCl₂ and 0.01% Tween-20 (50 μl per well) at pH 7.6 and room temperature for 4 h at 10 different concentrations. Subsequently, the wells were washed and incubated with HRP conjugate and 2% BSA in 25 mM HEPES with 150 mM NaCl, 5 mM CaCl₂ and 0.01% Tween-20 (50 μl) at pH 7.6 and room temperature for 45 min. The wells were washed and developed with TMB solution (Rockland) (50 μl per well). The reaction was quenched after 5 min by addition of 0.18 M sulfuric acid (50 μl per well). Binding of the Langerin ECD was detected via absorbance A₄₅₀ measurements at 450 nm using a SpectraMax spectrometer (Molecular Devices) in three independent titrations.

Cell Culture

THP-1 and Raji cells (ATCC) were cultured in RPMI1640 medium (Sigma Aldrich) containing 10% FCS (Biochrom), 100 U*ml⁻¹ penicillin and streptomycin (Life Technologies) and GlutaMax-I (Life Technologies). Langerin⁺ COS-7 cells (ATCC) were cultured in DMEM supplemented with 10% FCS (Pan-Biotech). Primary epidermal cells were cultured in RPMI1640 medium (Sigma Aldrich) supplemented with 10% FCS (Life Technologies), GlutaMax-I (Life Technologies), 50 µg/ml Gentamicin (Gibco) and 200 U/ml human GM-CSF (PeproTech). All cell lines were maintained at 5% CO₂ and 37°C.

Establishment of C-Type Lectin⁺ Model Cells

Lentivirus production. TrueORF sequence-validated cDNA clones of human Langerin, human DC-SIGN and murine Dectin-1 (Sinobiologicals) were amplified from a pcDNA5/FRT/V5-His-TOPO TA expression vector (Life Technologies) by PCR (forward primer: 5'- CTGGCTAGCGTTTAAACTT AAG -3', reverse primer: 5'-CAATGGTGATGGTGATGATG -3') using Phusion polymerase (Thermo Fisher Scientific). The PCR amplicons were cloned by Gibson assembly (NEB) according to the manufacturer's protocol in a BIC-PGK-Zeo-T2a-mAmetrine:EF1A construct that was linearized by PCR (forward primer: 5'-GAGCTAGCAGtaTTAATTAACCACCCTGGCTAGCGTTTAACTTAAG-3'; reverse primer: 5'-GTACCGGTTAGGATGCATGCCAATGGTGATGGTGATGATG -3') using Phusion Polymerase. Together with third-generation packaging vectors pVSV-G, pMDL and pRSV, the constructs were transfected into HEK293T cells (ATCC) using the Mirus LT1 reagent (Sopachem) for production of the lentivirus as previously published³⁶. After 3 to 4 days the supernatants containing the viral particles were harvested and frozen at -80°C to kill any remaining HEK293T cells. This supernatant was used to transduce Langerin, DC-SIGN and Dectin-1 into THP-1, Raji or COS-7 cells.

Lentiviral transduction. 50,000 THP-1, Raji or COS-7 cells were transduced by spin infection for 2 h at 1000 g and 33°C using 100 µl virus-containing supernatant supplemented with 8 µg/ml polybrene (Santa Cruz Biotechnology). The corresponding medium for the cell lines was added after centrifugation. 2 to 3 days post-transduction mAmetrine expression was measured by flow cytometry to confirm integration of the construct. Cells were selected 3 days post-infection by 100 µg/ml zeocin (Gibco) for THP-1 and COS-7 cells or 200 µg/ml for Raji cells. After selection, 95% of cells were mAmetrine⁺ and the expression of Langerin, DC-SIGN or Dectin-1 was validated by flow cytometry.

Preparation of Epidermal and Whole Skin Cell Suspensions

Healthy human skin samples were collected after informed consent and approval by the local ethics committee (AN 5003 360/5.22 of the 15.04.2016). Subcutaneous fat was removed with a scalpel. For preparation of epidermal cell suspension, skin pieces were incubated in RPMI1640 medium (Lonza)

containing 1.5 U/ml dispase II (Roche, Switzerland) and 0.1% trypsin (Sigma Aldrich) overnight at 4°C. Next the epidermis was isolated, broken up into smaller pieces, and filtered through a 100 µm cell strainer (Thermo Fisher Scientific) to obtain a single cell suspension. For digestion of whole skin, skin pieces were incubated in RPMI1640 medium (Lonza) supplemented with 10% FCS (Pan-Biotech) containing 1 mg/ml collagenase IV (Worthington Biochemical Corporation) overnight at 37°C. Cell suspension was then filtered through 40 µm and 100 µm cell strainer (Thermo Fisher Scientific).

Enrichment of CD1a⁺ epidermal cells

CD1a expressing epidermal cells were enriched from epidermal cell suspensions by magnetic labeling with human anti-CD1a MicroBeads (Miltenyi) and subsequent positive-selection by running LS MACS columns (Miltenyi) twice according to the manufacturer's instructions.

Flow Cytometry

C-type lectin receptor⁺ model cells. To validate the expression of CLR, 50,000 THP-1, Raji or COS-7 cells were incubated with 25 µl of the corresponding medium for the cell line containing fluorophore-labeled antibodies for Langerin (clone DCGM4, Beckman Coulter), DC-SIGN (clone 9E9A8, Bio Legend) or Dectin-1 (clone BG1FPJ, eBioscience). Isotype-matched antibodies were used for control experiments. After incubation for 30 min at 4°C, cells were washed and CLR expression was evaluated by flow cytometry on a FACS Canto II Flow Cytometer (BD Biosciences) and analyzed in FlowJo³⁷.

To monitor internalization and binding, liposomes and, in case of control experiments, 10 mM EDTA or 50 µg·ml⁻¹ mannan in PBS were added to 96 well microtiter plates (Nunc). For control experiments with EDTA, Langerin⁺ and DC-SIGN⁺ cells were preincubated with EDTA for 15 min at 4°C before the addition of liposomes to ensure the quantitative chelation of Ca²⁺ ions. Raji cells were counted, centrifuged at 500 g for 3 min, aspirated and resuspended in culture medium at 37° C and 5% CO₂. 50,000 cells were added to the 96 well microtiter plates (Nunc) to obtain a final volume of 100 µl. The plates were incubated for 1 h at 4° C and subsequently centrifuged at 500 g for 3 min. Cells were aspirated and resuspended in culture medium at 37° C and 5% CO₂. Internalization and binding of liposomes were evaluated by flow cytometry on an Attune Nxt Flow Cytometer equipped with an autosampler (Life Technologies) and analyzed with FlowJo³⁷. Following the initial optimization of the liposome concentration, all experiments were conducted at a total lipid concentration [Lipid]_T of 16 µM.

To evaluate cytotoxic effects induced by liposomes, Raji cells were stained with the early apoptotic marker Annexin-V and the late apoptotic marker 7-AAD. 10,000 cells were incubated with at different total lipid concentration [Lipid]_T for 24 h or at an [Lipid]_T of 16 µM for various times at a final volume of 50 µl at 37°C and 5% CO₂. Incubation with 50% DMSO for 3 min at the same condition was used

as a positive control. Following incubation, the cells were washed and resuspended in 25 μ l 10 mM HEPES with 140 mM NaCl and 2.5 mM CaCl_2 containing Annexin-V-FITC (1:100 dilution, Adipogen) at pH 7.4. Next, the cells were protected from light and incubated for 10 min at room temperature. After washing, the cells were resuspended in 100 μ l 10 mM HEPES with 140 mM NaCl and 2.5 mM CaCl_2 containing 7-AAD (1:100 dilution, Bio Legend) at pH 7.4, protected from light and incubated for 5 to 10 min at room temperature. Cytotoxic effects induced by liposomes were evaluated by flow cytometry on an Attune Nxt Flow Cytometer equipped with an autosampler (Life Technologies) and analyzed with FlowJo³⁷.

Epidermal and whole skin cell suspensions. Liposomes were incubated with epidermal or whole skin cell suspensions at a total lipid concentration $[\text{Lipid}]_T$ of 16 μ M in HBSS with 2 mM CaCl_2 (Biochrom) supplemented with 1% BSA (Serva Electrophoresis) for 1h at 37° C. For experiments analyzing the kinetics of liposome internalization, epidermal cell suspensions were incubated for varying times at 4° C or 37° C and endocytosis was abrogated by addition of 10 mM EDTA. Alternatively, liposomes were incubated for varying times at 4° C or 37° C with epidermal cell suspension in presence of 10 mM EDTA. To evaluate cytotoxicity or maturation effects induced by liposomes, epidermal cell suspensions were incubated with liposomes at an $[\text{Lipid}]_T$ of 2.5 μ M for 1h or 48h at 37°C in RPMI1640 medium (Lonza) supplemented with 10% FCS (Pan-Biotech), 2 mM L-glutamine (Lonza), 50 μ g/ml gentamicin (Gibco) and 200U/ml GM-CSF (Leukine sargramostim, Sanofi).

Flow cytometry experiments were conducted on a FACS Canto II Flow Cytometer (BD Biosciences) and analyzed in FlowJo³⁷. Non-specific FcR-mediated antibody staining was blocked by human FcR Blocking reagent (Miltenyi Biotec). Dead cells were excluded by the fixable viability dye eFluor 780 (eBioscience). Fluorophore-labeled primary antibodies for CD1a (clone HI149), CD14 (clone HCD14), HLA-DR (clone L243), CD45 (clone HI30), CD83 (clone HB15) (Bio Legend), CD80 (clone L307.4, BD Biosciences) and Langerin (clone MB22-9F5, Miltenyi Biotec) or isotype-matched control antibodies were used for gating. Immune cells were always pre-gated on viable CD45⁺ cells. All antibody incubation steps were performed for 15 min at 4° C. For intracellular staining of active caspase 3, staining was done according to the manufacturer's protocol and the cells were incubated with an antibody for active caspase 3 (clone C92-605; BD Biosciences) for 30 minutes at room temperature.

Cytokine ELISA

To assess the immunogenicity of targeted and non-targeted liposomes, a human TNF- α ELISA MAXTM (BioLegend) was performed according to the manufacturer's instructions. Briefly, 20,000 enriched CD1a⁺ epidermal cells were co-cultured with liposomes at a total lipid concentration $[\text{Lipid}]_T$ of 16 μ M lipid concentration in a final volume of 100 μ l culture medium for 15 h at 37°C and 5%

CO₂. The positive control was co-cultured with 20 µg/ml poly I:C (Sigma Aldrich) and 100 ng/ml LPS (Invivogen), whereas the negative control remained untreated. After centrifugation at 400 g for 5 min the supernatant was analyzed in the TNF-α ELISA.

Colorimetric Cytotoxicity Assay

To assess the cytotoxicity of doxorubicin-containing liposomes with THP-1 cells, 50,000 cells per well were added to 96 well microtiter plates (Corning) and incubated in presence of liposomes at a given total lipid concentration [Lipid]_T in a final volume of 100 µl for 48 h at 37°C and 5% CO₂. Cell viability was analyzed using CellTiter 96 (Promega) by measuring formazan absorbance at 490 nm. Complete killing was defined as the signal measured after cell lysis using 0.5 Triton X-100 and maximum viability was defined by conducting the experiment in absence of liposomes and doxorubicin.

Confocal Microscopy

C-type lectin receptor⁺ model cell lines. To analyze the co-localization of liposomes **22** with endosomal markers, cells were either stained by immunofluorescence in case of EEA1 and Rab5 or transfected with a YFP-Rab9 construct. The YFP-Rab9 construct was a kind gift of Dr. Oliver Rocks (Max Delbrück Centrum, Berlin)³⁸. Cells were seeded on glass coverslips in a 12-well tissue culture dish (Sigma Aldrich) and incubated with liposomes **22** at a total lipid concentration [Lipid]_T of 16 µM in DMEM at 4°C for 2h. Incubation was started either 1 day after seeding for staining by immunofluorescence or 1 day after transfection. For the initial time point, cells were washed with PBS with 2 mM MgCl₂ and 2 mM CaCl₂ (Invitrogen) at 4°C and fixed in 4% Roti-Histofix (Roth) for 10 min at room temperature. For the remaining time points, cells were incubated at 37°C, washed with PBS with 2 mM MgCl₂ and 2 mM CaCl₂ (Invitrogen) and subsequently fixed. For immunofluorescence, cells were washed 2 times with PBS and permeabilized in PBS with 0.2% Triton-X-100 and 100 mM glycine for 10 min at room temperature. After washing two times and subsequent blocking with PBS with 3% BSA for 30 min at room temperature, cells were incubated with primary antibodies for EEA1 (rabbit, clone C45B10) and Rab5 (rabbit, clone C8B1) (Cell Signaling Technology) in PBS with 3% BSA for 1h at room temperature. After washing three times for 5 min with PBS, cells were incubated with fluorophore-labeled secondary antibody (Invitrogen) for 30 min at room temperature followed by three additional washing steps. DAPI (1:1000 dilution, Thermo Fisher Scientific) in PBS was incubated for 5 min at room temperature, following by washing with PBS for 5 min at room temperature. Coverslips were mounted using Roti-Mount (Roth). For Rab9 visualization, cells were transfected 1 day after seeding with 500 ng YFP-Rab9 per well using Lipofectamine 2000 (Invitrogen) according to the manufacturer's protocol. After 1 day, cells were incubated with liposomes and fixed as described above. After fixation, cells were washed two times

with PBS and mounted. The co-localization of liposomes with endosomal markers was visualized with an SP8 confocal microscope (Leica).

Epidermal cell suspensions. For confocal microscopy, 100,000 cells obtained from an epidermal cell suspension in 200 μ l of RPMI1640 medium (Lonza) supplemented with 10% FCS (Pan-Biotech), 2 mM L-glutamine (Lonza) and 50 μ g/ml gentamicin (Gibco) were incubated with FITC-labeled CD1a (clone HI149, Bio Legend) in a micro-slide 8 well (Ibidi) for 15 minutes at 4° C. Next, the cells were incubated for 1 h with liposomes **22** at a total lipid concentration [Lipid]_T of 16 μ M at 37° C. Internalization of liposomes was visualized with an AxioObserver Z1 confocal microscope (Carl Zeiss).

Statistical Analysis

For all figures, error bars reflect the standard error of the mean. For Figure 4, the repeated One-Way ANOVA Test with a post-hoc Tukey's Test was employed for statistical analysis. The analysis was conducted independently for the 1 h and 48 h time points.

Supporting References

1. Hanske, J.; Aleksic, S.; Ballaschk, M.; Jurk, M.; Shanina, E.; Beerbaum, M.; Schmieder, P.; Keller, B. G.; Rademacher, C., Intradomain allosteric network modulates calcium affinity of the C-type lectin receptor Langerin. *J Am Chem Soc* **2016**, *138* (37), 12176-12186.
2. Hanske, J.; Wawrzinek, R.; Geissner, A.; Wamhoff, E. C.; Sellrie, K.; Schmidt, H.; Seeberger, P. H.; Rademacher, C., Calcium-independent activation of an allosteric network in Langerin by heparin oligosaccharides. *ChemBioChem* **2017**, *18* (13), 1183-1187.
3. Wamhoff, E. C.; Hanske, J.; Schnirch, L.; Aretz, J.; Grube, M.; Varon Silva, D.; Rademacher, C., 19F NMR-guided design of glycomimetic Langerin ligands. *ACS Chem Biol* **2016**, *11* (9), 2407-2413.
4. Carr H. Y.; M., P. E., Effects of diffusion on free precession in nuclear magnetic resonance experiments. *Phys Rev* **1954**, *94* (3), 630-638.
5. Meiboom, S.; Gill, D., Modified spin - echo method for measuring nuclear relaxation times. *Rev Sci Instrum* **1958**, *29* (8), 688-691.
6. Holla, A.; Skerra, A., Comparative analysis reveals selective recognition of glycans by the dendritic cell receptors DC-SIGN and Langerin. *Protein Eng Des Sel* **2011**, *24* (9), 659-669.
7. Feinberg, H.; Rowntree, T. J.; Tan, S. L.; Drickamer, K.; Weis, W. I.; Taylor, M. E., Common polymorphisms in human Langerin change specificity for glycan ligands. *J Biol Chem* **2013**, *288* (52), 36762-36771.
8. Feinberg, H.; Taylor, M. E.; Razi, N.; McBride, R.; Knirel, Y. A.; Graham, S. A.; Drickamer, K.; Weis, W. I., Structural basis for langerin recognition of diverse pathogen and mammalian glycans through a single binding site. *J Mol Biol* **2011**, *405* (4), 1027-1039.
9. Ellervik, U.; Magnusson, G., Glycosylation with N-Troc-protected glycosyl donors. *Carbohydr Res* **1996**, *280* (2), 251-260.
10. Hayes, W.; Osborn, H. M. I.; Osborne, S. D.; Rastall, R. A.; Romagnoli, B., One-pot synthesis of multivalent arrays of mannose mono- and disaccharides. *Tetrahedron* **2003**, *59* (40), 7983-7996.
11. Petersen, B. O.; Vinogradov, E.; Kay, W.; Wurtz, P.; Nyberg, N. T.; Duus, J. O.; Sorensen, O. W., H2BC: a new technique for NMR analysis of complex carbohydrates. *Carbohydr Res* **2006**, *341* (4), 550-556.
12. Duus, J.; Gotfredsen, C. H.; Bock, K., Carbohydrate structural determination by NMR spectroscopy: modern methods and limitations. *Chem Rev* **2000**, *100* (12), 4589-4614.
13. Mestrelab Research *MestreNova*, 11.0.2; 2016.
14. Aretz, J.; Wamhoff, E. C.; Hanske, J.; Heymann, D.; Rademacher, C., Computational and experimental prediction of human C-type lectin receptor druggability. *Front Immunol* **2014**, *5*, 323.
15. OriginLab *OriginPro*, 9.1; 2015.
16. Bodenhausen, G.; Ruben, D. J., Natural abundance nitrogen-15 NMR by enhanced heteronuclear spectroscopy. *Chem Phys Lett* **1980**, *69* (1), 185-189.

17. Delaglio, F.; Grzesiek, S.; Vuister, G. W.; Zhu, G.; Pfeifer, J.; Bax, A., NMRPipe: a multidimensional spectral processing system based on UNIX pipes. *J Biomol NMR* **1995**, *6* (3), 277-293.
18. Vranken, W. F.; Boucher, W.; Stevens, T. J.; Fogh, R. H.; Pajon, A.; Llinas, M.; Ulrich, E. L.; Markley, J. L.; Ionides, J.; Laue, E. D., The CCPN data model for NMR spectroscopy: development of a software pipeline. *Proteins* **2005**, *59* (4), 687-696.
19. MathWorks *MatLab*, 9.0; Natick, U.S.A., 2016.
20. Liu, M.; Mao, X.-a.; Ye, C.; Huang, H.; Nicholson, J. K.; Lindon, J. C., Improved WATERGATE pulse sequences for solvent suppression in NMR spectroscopy. *J Magn Reson* **1998**, *132* (1), 125-129.
21. Williamson, M. P., Using chemical shift perturbation to characterise ligand binding. *Prog Nucl Magn Reson Spectrosc* **2013**, *73*, 1-16.
22. MathWorks *Bioinformatics Toolbox*, 4.7; Natick, U.S.A., 2016.
23. ChemicalComputingGroup *Molecular Operating Environment*, 2016.08; Montreal, Canada, 2016.
24. Connolly, M. L., The molecular surface package. *J Mol Graph* **1993**, *11* (2), 139-141.
25. Mayer, M.; Meyer, B., Characterization of ligand binding by Saturation Transfer Difference NMR spectroscopy. *Angew Chem Int Ed* **1999**, *38* (12), 1784-1788.
26. Hwang, T. L.; Shaka, A. J., Water suppression that works - excitation sculpting using arbitrary wave-forms and pulsed-field gradients. *J Magn Reson* **1995**, *112* (2), 275-279.
27. Sklenar, V.; Piotto, M.; Leppik, R.; Saudek, V., Gradient-tailored water suppression for 1H-15N HSQC experiments optimized to retain full sensitivity. *J Magn Reson* **1993**, *102* (2), 241-245.
28. Mayer, M.; Meyer, B., Group epitope mapping by saturation transfer difference NMR to identify segments of a ligand in direct contact with a protein receptor. *J Am Chem Soc* **2001**, *123* (25), 6108-6117.
29. Angulo, J.; Nieto, P. M., STD-NMR: application to transient interactions between biomolecules-a quantitative approach. *Eur Biophys J* **2011**, *40* (12), 1357-1369.
30. Case, D. A., Darden, T. A., Cheatham, T. E., Simmerling, C. L., Wang, J., Duke, R. E., Luo, R., Crowley, M., R.C.Walker, Zhang, W., Merz, K. M., B.Wang, Hayik, S., Roitberg, A., Seabra, G., Kolossváry, I., K.F.Wong, Paesani, F., Vanicek, J., X.Wu, Brozell, S. R., Steinbrecher, T., Gohlke, H., Yang, L., Tan, C., Mongan, J., Hornak, V., Cui, G., Mathews, D. H., Seetin, M. G., Sagui, C., Babin, V. and P.A. Kollman *AMBER*, 10; San Francisco, U.S.A., 2008.
31. Gerber, P. R.; Muller, K., MAB, a generally applicable molecular force field for structure modelling in medicinal chemistry. *J Comput Aided Mol Des* **1995**, *9* (3), 251-268.
32. Halgren, T. A., Merck molecular force field. I. Basis, form, scope, parameterization, and performance of MMFF94. *J Comput Chem* **1996**, *17* (5-6), 490-519.
33. Corbeil, C. R.; Williams, C. I.; Labute, P., Variability in docking success rates due to dataset preparation. *J Comput Aided Mol Des* **2012**, *26* (6), 775-786.
34. Chen, W. C.; Completo, G. C.; Sigal, D. S.; Crocker, P. R.; Saven, A.; Paulson, J. C., In vivo targeting of B-cell lymphoma with glycan ligands of CD22. *Blood* **2010**, *115* (23), 4778-4786.
35. Fehres, C. M.; Kalay, H.; Bruijns, S. C.; Musaafir, S. A.; Ambrosini, M.; van Bloois, L.; van Vliet, S. J.; Storm, G.; Garcia-Vallejo, J. J.; van Kooyk, Y., Cross-presentation through Langerin and

DC-SIGN targeting requires different formulations of glycan-modified antigens. *Journal of controlled release : official journal of the Controlled Release Society* **2015**, *203*, 67-76.

36. van de Weijer, M. L.; van Muijlwijk, G. H.; Visser, L. J.; Costa, A. I.; Wiertz, E. J.; Lebbink, R. J., The E3 ubiquitin ligase TMEM129 is a tri-spanning transmembrane protein. *Viruses* **2016**, *8* (11), 309.

37. TreeStar *FlowJo*, 10.0.7; San Francisco, U.S.A., 2017.

38. Colwill, K.; Wells, C. D.; Elder, K.; Goudreault, M.; Hersi, K.; Kulkarni, S.; Hardy, W. R.; Pawson, T.; Morin, G. B., Modification of the Creator recombination system for proteomics applications - improved expression by addition of splice sites. *BMC Biotechnol* **2006**, *6* (13).